

# Cognitive Sustainability

Sep 2023

Vol. 2 | No. 3 | ISSN 2939-5240



## Cognitive Sustainability

Cognitive Sustainability (CogSust) is a double-blind peer-reviewed scientific journal published by CogSust Ltd.  
(H1116 Budapest Putnok u 9.)

The person responsible for publishing: Mária Szalmáné Csete [editor@cogsust.com](mailto:editor@cogsust.com)

The person responsible for editing: Ádám Török [info@cogsust.com](mailto:info@cogsust.com)

CogSust is an online quarterly journal, publication frequency: quarterly, by March, June, September, December.

**ISSN 2939-5240**

This journal uses a license: Attribution-NonCommercial-ShareAlike 4.0 International (CC BY-NC-SA 4.0)

The journal is indexed by:



Library of Hungarian Scientific Works




Repository of the Library of Hungarian Academy of Science



# Sustainable operation? Measuring the actual consumption of a hybrid car and determining its consumption curve

Imre Zsombók

 0000-0002-6073-1732

*AK-S Ltd.*

Budapest, Hungary

zsombok@ak-s.hu

## Abstract

Sustainability is one of the most commonly used terms concerning renewable energy, environmental protection and energy management. Without a doubt, understanding its full meaning, it is clear that sustainability is paramount for the quality of life of future generations and for the Earth as a living space. The presented work aims to give an overview of the importance of on-board management in hybrid vehicles as an important tool to increase their contribution to sustainable mobility. Real-world condition measurements were carried out based on the available cognitive features of an average vehicle. Several main consumers were also tested to present their role within cognitive and sustainable mobility. Results show that there is a function between the battery load level and the hybrid vehicle electric power use likeliness. Among the primary but under-addressed concerns today are the uninhibited exploitation of non-renewable energy sources and the avoidance of pollution.

## Keywords

sustainability, climate changes, vehicle industry, waste reduction

## 1 Introduction

The automotive industry is one of the largest emitters during manufacturing, considering any technology, and during the product's life cycle. The car industry is trying to become more sustainable in several ways. These include:

- Electric vehicles (EVs): electric cars are powered by an electric motor instead of a conventional combustion engine. EVs could be environmentally friendly during use, as they do not emit pollutants in the direct exhaust. EVs can reduce greenhouse gas emissions long-term if energy production comes from clean sources.
- Hybrid vehicles: hybrid cars combine internal combustion engines and electric motors. Hybrid systems enable improved fuel efficiency and reduced emissions. Such vehicles can operate quietly and in an environmentally friendly way on short journeys with an electric motor, while on longer journeys, the combustion engine provides the power (*Koller et al. 2022*).
- Fuel cell vehicles: fuel cell cars use hydrogen as fuel, which is converted into electricity in fuel cells. This produces clean water vapour as an emission. Fuel cell vehicles can provide longer range and faster recharging than electric cars (*Chechresaz, 2013*).
- Use of environmentally friendly materials: car manufacturers increasingly use environmentally friendly materials to make cars. For example, they apply more recycled materials, bio-based plastics and lightweight metals, which reduce the ecological footprint of cars.
- Improving the efficiency of manufacturing processes: in the automotive industry, improving the efficiency of manufacturing processes also contributes to bringing the industry closer to sustainability. Using energy, raw materials and waste in manufacturing significantly impacts the environment and society (*Yang et al., 2014*).



## 2 Background

Over the last decades, developed countries have taken several measures to reduce emissions of greenhouse gases and soil and groundwater pollutants, mainly for economic reasons but also for human comfort, with varying degrees of success.

The EURO emission standards are widely used, and they are the drivers of drivetrain development regulations in the automotive industry, which are summarised in the list below:

- Euro 1 (1992):
  - For passenger cars-91/441/EEC (*Da Costa et al., 2012*).
  - Also, for passenger cars and light lorries-93/59/EEC.
- Euro 2 (1996) for passenger cars-94/12/EC (96/69/EC)
  - For motorcycle-2002/51/EC (row A)
- Euro 3 (2000) for any vehicle-98/69/EC (*Chehresaz, 2013*)
  - For motorcycle-2002/51/EC (row B)
- Euro 4 (2005) for any vehicle (98/69/EC & 2002/80/EC)
- Euro 5 (2009) for light passenger and commercial vehicles (715/2007/EC)
- Euro 6 (2014) for light passenger and commercial vehicles (459/2012/EC and 2016/646/EU)
- Euro 7 (probably 2025).

The EURO 7 regulation is not expected to introduce any significant tightening compared to the previous stage but puts petrol and diesel cars on an equal footing. As far as we know, this regulation will be in place until the end of 2034, when it will be replaced by new EU legislation from 2035, requiring new cars placed on the market to be zero-emission. Of course, the unplanned development of technology or the insufficient development of the electric grid and, in this case, charging points could mean a postponement of the introduction of the regulation.

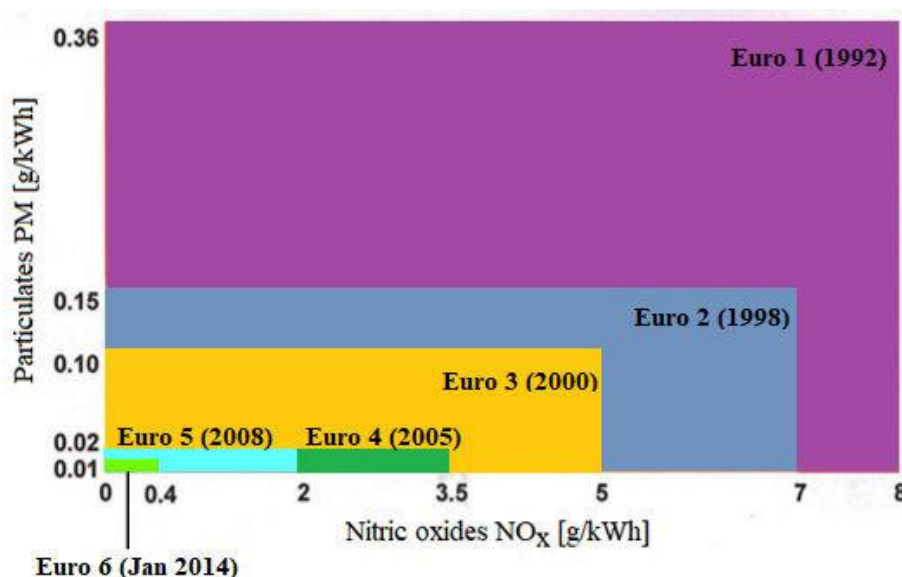


Figure 1. EURO 1–6 emission standards PM/NO<sub>x</sub>

Source: Jurchiş, et al., 2018

Sustainability in all areas of the automotive industry is becoming extremely important, and, as a result, the automotive industry is undergoing a radical transformation. Four main trends drive this transformation: electric mobility, shared mobility services, autonomous driving and connected vehicles. The growing interest in electric cars and innovative mobility concepts shows how sustainability has become a key issue. At the same time,



developers and investors are also paying increasing attention: they want to understand the risks and threats faced by car manufacturers and suppliers and, simultaneously, avoid the loss of prestige associated with non-climate-friendly companies.

This development is being accelerated by both political requirements and changing consumer preferences. Some manufacturers and suppliers have implemented these trends, at least to some extent. For example, they are increasing their fleet of electric vehicles and offering flexible mobility concepts. However, the opportunities are far from exhausted: transforming the automotive industry into a truly sustainable industry is still a long way off (*Zöldy, 2009*).

As far as energy efficiency is concerned, car manufacturers are increasingly improving their energy efficiency. This may include using more efficient machinery and equipment, using renewable energy sources for production processes, and recovering waste heat and wastewater.

Three main themes characterise this development:

1. Climate change and CO<sub>2</sub> emissions

Climate change and its impacts have long been the subject of widespread public debate. As a result, legislators have significantly tightened CO<sub>2</sub> emission standards in recent years. Car manufacturers must reduce CO<sub>2</sub> emissions from vehicle production and the fleet. In this context, using alternative powertrains such as fuel cells, electric drives, and hybrid drives plays an important role.

2. Sustainability of the value chain

As natural resources become scarce, sustainable value chains are becoming increasingly important for the automotive industry. They are based on the principle of resource reuse and recycling. It is particularly important to create transparency along the supply chain. Only then can the origin of components be traced and sustainability ensured along the entire value chain. In this light, car manufacturers and suppliers are working on innovative concepts such as the circular economy, battery recycling, biodegradable components and sustainable processes in research, development and manufacturing.

3. Digital Responsibility

With the increasing uptake of autonomous and connected vehicles, issues such as digital value creation, privacy and data security are coming to the fore. On the one hand, automotive manufacturers and suppliers must define the digital features and technologies needed to deliver sustainable solutions. On the other hand, strict policies are needed to prevent data breaches.

### 3 Test methods

Our research focused on exploring a solution, the hybrid drive, which is regarded as a sustainable alternative in the short to medium term, both environmentally and economically. Plug-in hybrid drive vehicles (PHEV) are the ones that come close to the desired goals at an affordable price and with lower emissions (*Yang et al., 2014*).

The key of the presented research is to measure the energy flow on the vehicle. There are many different ways and many different methods to determine the consumption of vehicles. The purpose of determining average fuel consumption is to inform the customer of the approximate fuel costs of maintaining the chosen vehicle and to determine the vehicle's emissions based on this value. These theoretical procedures, however, do not consider several factors that may distort emissions and fuel consumption figures in real-life conditions (*Zöldy, 2019*).

The most commonly used fuel consumption and emission measurement methods are presented in the next chapter. They serve as a benchmark for the test carried out.

The New European Driving Cycle (NEDC) was the first driving cycle model to become widespread. It was developed in the 1970s and updated with empirical knowledge. The last update was in 1997 but was still used in 2019 (Koller *et al.*, 2022).

The year-by-year faster development in the automotive industry requires a new measurement model; driving habits have changed, requiring longer distances over a wider geographical area, better quality roads, and larger road networks; average speeds have become significantly higher, and modern cars have become larger and heavier (Zsombok, Zöldy, 2023). The NEDC measurement cycle is two-phase: urban and ‘extra-urban’. The test assumed an ideal, calm environment, which led to erroneous results.

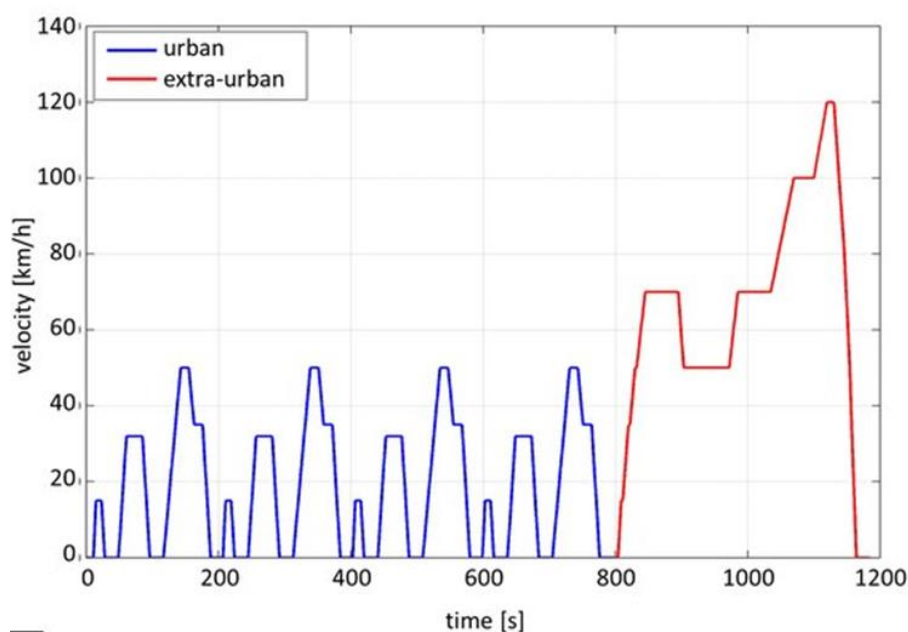


Figure 2. NEDC travel cycle speed-time diagram.

Source: Koller *et al.*, 2022

#### 1. WLTP – Worldwide Harmonised Light Vehicles Test Procedure

By 2015, a new model was born that attempted to eliminate the flaws of the previous NEDC by providing a more realistic test protocol (Chehresaz, 2013; Williams *et al.*, 2011). The new cycle is 10 minutes longer (30 minutes instead of the previous 20 minutes), and the speed profile is more dynamic, with higher acceleration and longer braking distances. The average speed increased to 46.5 km/h, and the top speed to 131.3 km/h. The distance covered was 23.25 km, more than double that of the NEDC.

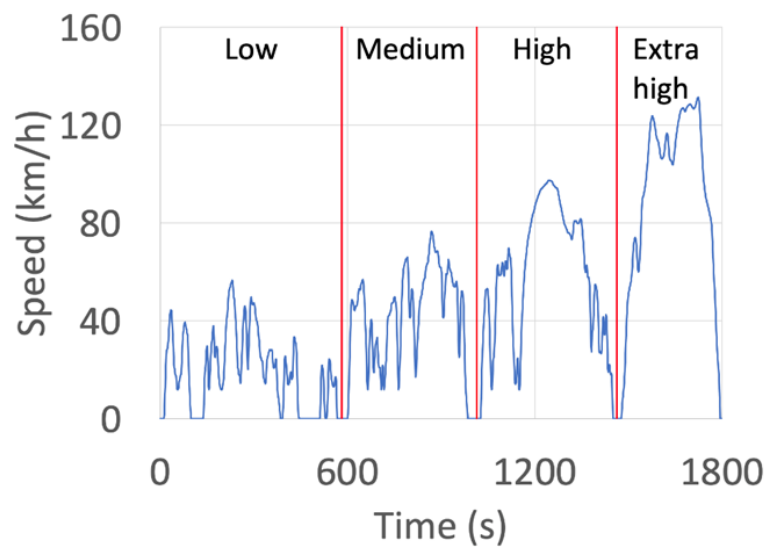


Figure 3: WLTP driving cycle speed-time diagram

Source: Yao, 2019

## 2. EPA Federal test procedure (FTP-75)

The US Environmental Protection Agency (EPA) standard, also known as FTP-75, is a more complex and, therefore, more realistic set of tests than the two listed above. It is not a new standard, as the first version was published in 1978, and the current one was updated in 2008. The current test cycle consists of 4 parts: urban stage (FTP-75), highway stage (HWFET), aggressive driving (SFTP US06) and optionally air conditioning stage (SFTP SC03). The FTP-75 test consists of 3 parts: cold start, transient phase, and warm start. The warm start phase is a repetition of the cold start, each lasting 505 seconds. To make the brake pad measurement a good approximation of real driving conditions, in 2007, the EPA added two additional tests to the standard. One is the US06, designed to replicate an aggressive driving style: high speeds, strong accelerations, and extreme speed curve changes. The test section lasts 10 minutes, covers 8 miles (13 km), has an average speed of 48 mph (77 km/h) and a maximum speed of 80 mph (130 km/h). The cycle includes four complete stops. The other additional cycle is SC03, the air conditioning phase. During the 9.9-minute stage, 3.6 miles (5.8 km) are covered at an average speed of 22 mph (35 km/h) with five complete stops. Stopping time accounts for 19% of the test.

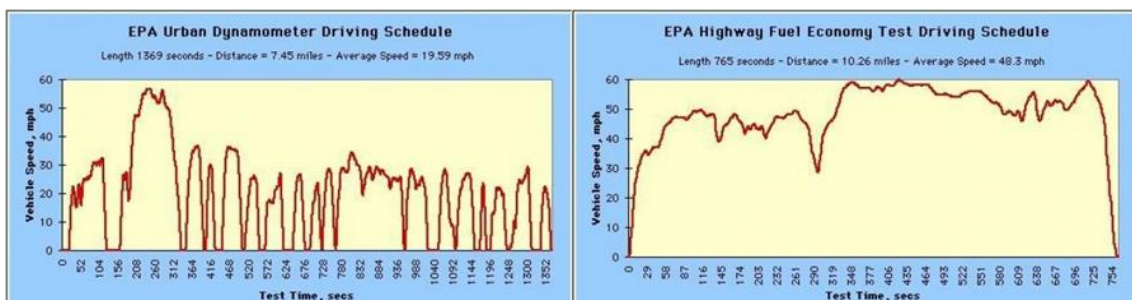


Figure 4: Speed-time diagram of urban and highway sections of the EPA driving cycle

Source: EPA, 2022



### 3. UF – Utility Factor

Plug-in hybrid vehicles (PHEVs) can operate in two basic modes: charge-depleting (CD) and charge-sustaining (CS). In CD mode, the vehicle drives the wheels purely electrically, using up the charge of the batteries. In contrast, in CS mode, an internal combustion engine powered by the combustion of various fuels (petrol, diesel, e-fuel) provides the propulsion while generating electricity through recuperative braking. The proportion of the total distance travelled by the vehicle in pure electric mode, i.e. CD mode, is indicated by the Utility Factor (UF) (Yang *et al.*, 2014).

In the European Union and in countries where the WLTP standard is still adopted, the UF can be calculated as follows (Eder *et al.*, 2014):

$$UF(AER, d_n) = 1 - \exp \left[ - \sum_{i=1}^{10} c_i \left( \frac{AER}{d_n} \right)^i \right]$$

where,

$AER$  is the pure electric range of the vehicle, according to WLTP;

$d_n$  is the distance, which in Europe is 800 km;

$c_i$  is the  $i^{\text{th}}$  coefficient (Table 1):

$C_1$	$C_2$	$C_3$	$C_4$	$C_5$
26.25	-38.94	-631.05	5964.83	-25095.60
$C_6$	$C_7$	$C_8$	$C_9$	$C_{10}$
60380.21	-87517.16	75513.77	-35748.77	7154.94

Table 1:  $i$ -th coefficient values

Source: Eder *et al.*, 2014

### 4 Sustainability concerns for hybrid vehicles

The plug-in hybrid electric drive (PHEV) is a powertrain comprising an electric motor and a conventional internal combustion engine. Their deployment is designed to reduce global greenhouse gas emissions and local air pollution in the least compromised, cost-effective way, but only if the electric drive operates near full capacity. PHEVs comprise around one-third of the global electric vehicle fleet, and their number is expected to grow. There is limited evidence that PHEVs are used as intended in everyday life and that the electric powertrain battery works properly, nor is there any measurement of how much conventional fuel is used. Reports have already been produced, considering user behaviour patterns in different countries. Around 100,000 PHEV vehicles in China, Europe and North America were included in the study (Plötz *et al.*, 2021).

In sum, on average, PHEV vehicles' fuel consumption and tailpipe CO<sub>2</sub> emissions under real driving conditions are about four times higher than type-approval values. This value is even more unfavourable when company vehicles are used.



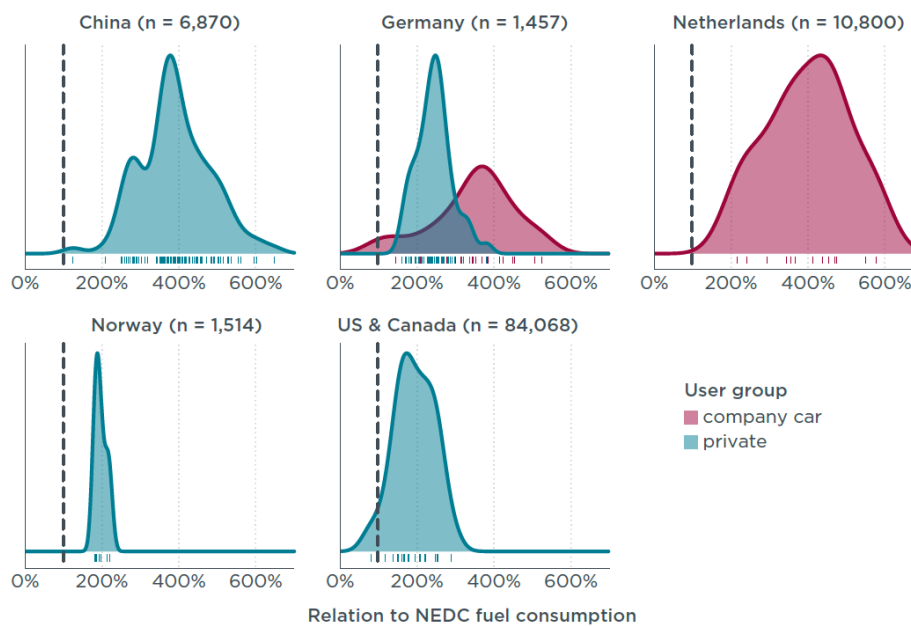


Figure 5: Real-world consumption of PHEV vehicles

Source: Plötz et al., 2021

In our measurement, we explored how the consumption and emissions of PHEV passenger cars evolve under the same traffic conditions, using different driving styles. The focus of the study is the less-researched question of the combined consumption curve of a complex hybrid system (Zalacko et al., 2020). From a sustainability perspective, considering the above findings and social research, it would be appropriate to set targets or development paths that end-users can adapt to in all circumstances. If these aspects are not considered, we will only have a semblance of results similar to the PHEV company car application (Da Costa et al., 2012).

## 5 Measurement

A Volkswagen Passat GTE passenger car registered in 2016 with 197,000 km already driven was used for the measurement. The vehicle has an unladen weight of 1765 kg and is equipped in line with the most sold versions. The vehicle is a parallel plug-in hybrid with an internal combustion engine of 1395 cm<sup>3</sup>, capable of delivering 115 kW of power according to factory specifications and 250 Nm of torque. The electric motor element of the powertrain has a power output of 85 kW and 350 Nm of torque. According to the manufacturer, the combined power output is 165 kW. The measurement did not consider the reduction in power resulting from the engine's running power.

Basic data obtained via OBD:

- Speed [km/h]
- Pedal position [%]
- Torque of electric motor [Nm]
- Battery voltage [V]
- Battery current [A]
- Electric motor power [kW]
- Battery state of charge (SOC) [%]
- Internal combustion engine speed [rpm]
- Internal combustion engine torque [Nm]
- Internal combustion engine load [%]
- Instantaneous fuel consumption [l/h]

Table 1. Measurement cycle data.



	Cycle 1			Cycle 2			Cycle 3			
section	City	highway	motorway	City	highway	motorway	City	highway	motorway	
passengers	2			2			2	1		
A/C	off			on			on			
mode	normal hybrid			normal hybrid		GTE	GTE	normal hybrid		GTE
average speed	27.49 km/h	49.39 km/h	105.49 km/h	30.23 km/h	49.67 km/h	103.205 km/h	24.48 km/h	48.82 km/h	103.45 km/h	
time	752.28 s	656.69 s	580.83 s	682.96 s	653.22 s	593.81 s	849.08 s	661.36 s	592.2 s	

The measurement aimed to obtain results comparable to currently available measurement cycles, but in contrast to them, not based on a blueprint, but on real conditions. Like Real Driving Emission (RDE) tests, Real-world Driving Cycle (RWDC) measurements are designed to further understand the unpredictability of traffic and certain vehicle characteristics through different driving styles. The consumption of the Volkswagen Passat GTE used in the measurement was tested on individually created tracks. The author created his measurement track. The evaluation is compared with catalogue data determined in the (WLTP EPA) measurements (Wiki Automotive Catalog, n.d.). When designing the measurement route, it was important to ensure that there was a sufficient length of flat, gently sloping expressway section, typical of most large European cities (as industrial centres). The length of the chosen route was planned to be 30-35 minutes, assuming normal traffic conditions and respecting speed limits.

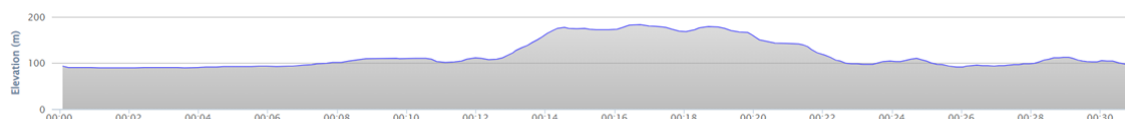


Figure 6. Elevation profile of the test route

In the measurement, we have sought to observe only those variables that are most typical for commuters. These were the air conditioning system, the variable weight, and slightly modifying the air resistance characteristics.

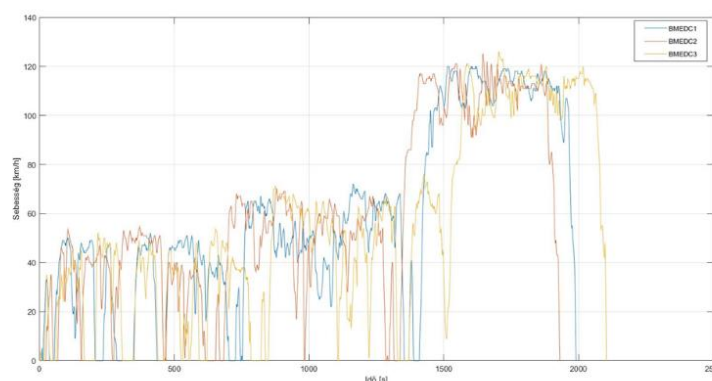


Figure 7. Speed profile during measurements

## 6 Results



As shown in the diagram below, the battery usage curve is similar in all three measurements due to the same path, but it can be seen that the system uses the available electrical energy more “bravely” when the charge is higher.

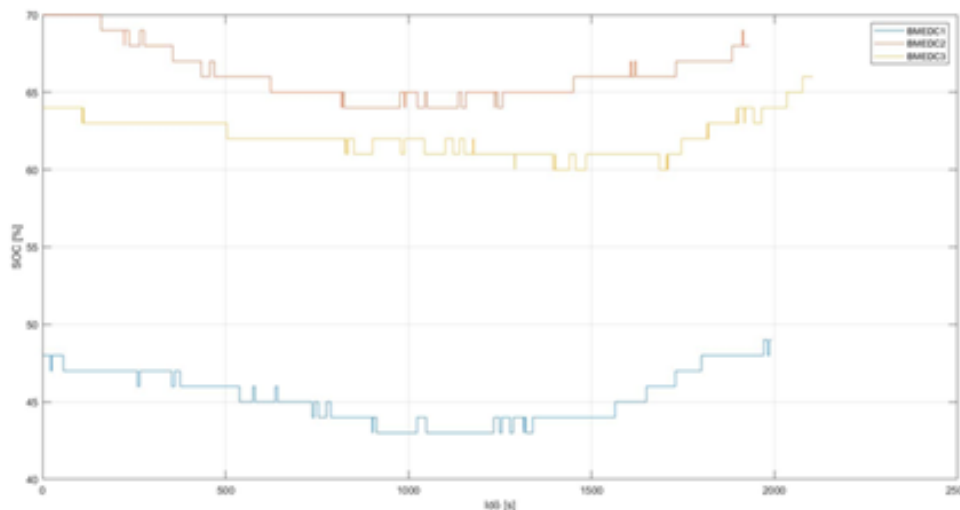


Figure 8. Variation of battery charge level during measurements

To determine the consumption, the instantaneous power of the drivetrain elements as a function of pedal depression was recorded during the measurement. We could also assign a speed to these values to determine the instantaneous consumption Eq. (1).

$$P = M * 2 * \pi * \frac{n}{60}, \tag{1}$$

where

$P$  – power;

$n$  – RPM;

$M$  – torque.

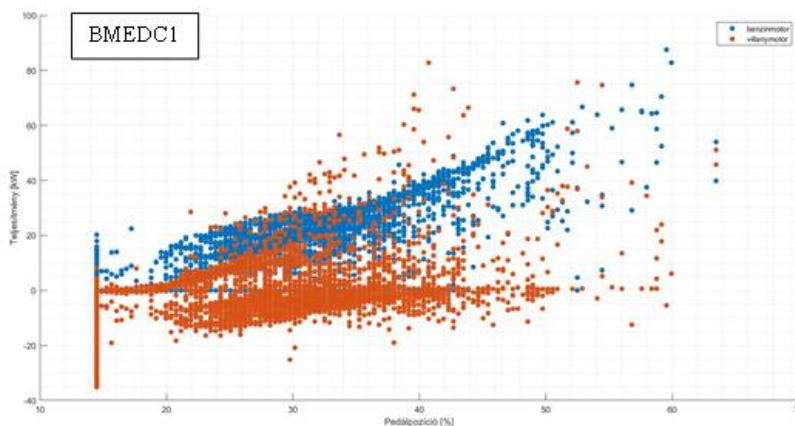


Figure 9. Performance of drive chain elements as a function of pedal position.

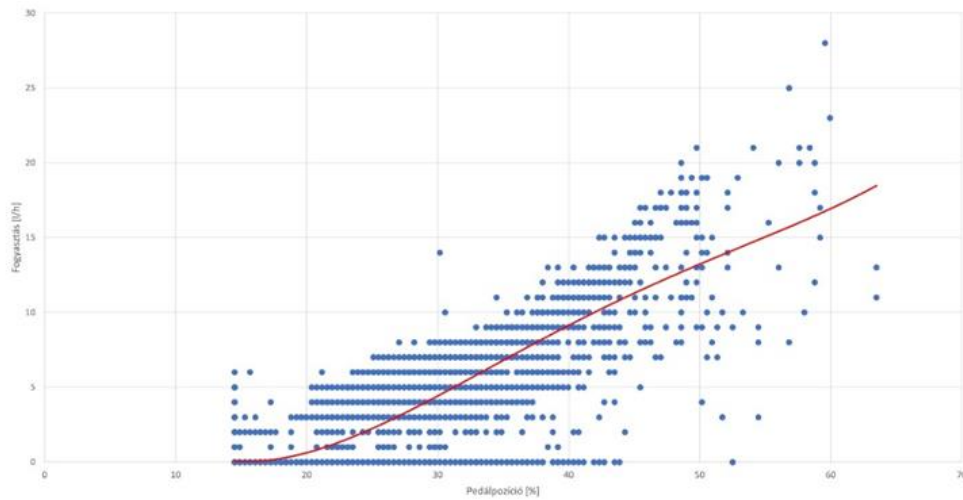


Figure 10. Instantaneous measured consumption.

## 7 Conclusion

Unfortunately, the energy consumption of the electric motor and the instantaneous consumption of the internal combustion engine could only be monitored separately, so evaluating the measurement and its adequacy would require further measurements. Even though we tried to follow the assumptions of the chassis dyno measurements both in the creation of the cycle and during its execution, the evaluation of the measurement cycles under real conditions provided results that require further investigation and deeper analysis. It can be concluded that, in real conditions, there is a deviation from the theoretical values. Even following the prescribed set of conditions, the vehicle consumption is higher. Hence, the emissions are higher (*Jurchiş et al., 2018*). Comparisons with WLTP or other driving cycle results are not fully possible, but based on the results, the following can be stated: if the battery charge level is higher, the hybrid system supports the combustion engine better, thus lowering consumption and emissions. The measurements show that the continuous utilisation of hybrid vehicles' electric drive in real driving conditions positively affects mobility sustainability.



## References

- Chehresaz, M. (2013). Modeling and design optimisation of plug-in hybrid electric vehicle powertrains. Master's thesis, University of Waterloo. Waterloo, Ontario, Canada. URL.: <https://core.ac.uk/download/pdf/144146911.pdf> (Downloaded: 21 April 2023)
- Da Costa, A., Kim, N., Le Berr, F., Marc, N., Badin, F., Rousseau, A. (2012). Fuel consumption potential of different plug-in hybrid vehicle architectures in the European and American contexts. *World Electric Vehicle Journal*. 5(1), 159–172. DOI: <https://doi.org/ktq5>
- Eder A., Schütze N., Rijnders A., Riemersma I., Steven H. (2014). Development of a European Utility Factor Curve for OVC-HEVs for WLTP. 2014 November. URL: [https://circabc.europa.eu/sd/a/92324676-bd8c-4075-8301-6caf12283beb/Technical%20Report\\_UF\\_final.pdf](https://circabc.europa.eu/sd/a/92324676-bd8c-4075-8301-6caf12283beb/Technical%20Report_UF_final.pdf) (Downloaded 23 September 2023)
- EPA – US Environmental Protection Agency. (2022). *Dynamometer Drive Schedules*. <https://www.epa.gov/vehicle-and-fuel-emissions-testing/dynamometer-drive-schedules>, (Downloaded 23 September 2023)
- Fuel consumption, electric driving, and CO<sub>2</sub> emissions. ICCT White Paper. URL: <https://theicct.org/publication/real-world-usage-of-plug-in-hybrid-electric-vehicles-fuel-consumption-electric-driving-and-co2-emissions/> (Downloaded 23 September 2023)
- Jurchiș, B. M., Burnete, N., Burnete, N. V., & Iclodean, C. D. (2018). Particulate matter emission characteristics for a compression ignition engine fueled with a blend of biodiesel and diesel. In IOP Conference Series: Materials Science and Engineering (Vol. 444, No. 7, p. 072012). IOP Publishing. DOI: <https://doi.org/ktq4>
- Jurchiș, B. M., Burnete, N., Burnete, N. V., Iclodean, C. D. (2018). Particulate matter emission characteristics for a compression ignition engine fueled with a blend of biodiesel and diesel. *Materials Science and Engineering*. 444(7), 072012). DOI: <https://doi.org/ktq4>
- Koller, T., Tóth-Nagy, C., Perger, J. (2022). Implementation of vehicle simulation model in a modern dynamometer test environment. *Cognitive Sustainability*, 1(4), DOI: <https://doi.org/gr2bds>
- Plötz, P., Moll, C., Bieker, G., Mock, P. (2021) Real-world usage of plug-in hybrid electric vehicles - Fuel consumption, electric driving, and CO<sub>2</sub> emissions URL: <https://theicct.org/wp-content/uploads/2021/06/PHEV-FS-EN-sept2020-0.pdf>
- Wiki Automotive Catalog (n.d.). 2019 Volkswagen Passat (B8, facelift 2019) GTE 1.4 TSI (218 Hp) Plug-in Hybrid DSG | Technical specs, data, fuel consumption, Dimensions. URL: <https://www.auto-data.net/en/volkswagen-passat-b8-facelift-2019-gte-1.4-tsi-218hp-plug-in-hybrid-dsg-41576> (Downloaded 23 September 2023)
- Williams, B., Martin, E., Lipman, T., Kammen, D. (2011). Plug-in-hybrid vehicle use, energy consumption, and greenhouse emissions: An analysis of household vehicle placements in Northern California. *Energies*. 4(3), 435–457. DOI: <https://doi.org/d9vv7j>
- Yang, Y., Jiang, W., Suntharalingam, P. (2014). Plug-in hybrid electric vehicles. In: Emadi, A. (ed.): *Advanced Electric Drive Vehicles*. CRC Press, Taylor and Francis Group, Boca Raton, FL, 465–490. DOI: <https://doi.org/ktq8>
- Yao, G., Du, C., Ge, Q., Jiang, H., Wang, Y., Ait-Ahmed, M., Moreau, L. (2019). “Traffic-Condition-Prediction-Based HMA-FIS Energy-Management Strategy for Fuel-Cell Electric Vehicles.” *Energies*, 12(23), p. 4426. DOI: <https://doi.org/kvn5>
- Zalacko, R., Zöldy, M., Simongáti, G. (2020). Comparative study of two simple marine engine BSFC estimation methods. *Brodogradnja*. 71(3), 13–25. DOI: <https://doi.org/hb7z>
- Zöldy, M. (2009). Potential future renewable fuel challenges for internal combustion engine. *Vehicles and Mobile Machines* [In Hungarian: *Járművek és Mobilgépek*]. 2(4), 397–403.
- Zöldy, M. (2019). Improving heavy-duty vehicles' fuel consumption with density and friction modifiers. *International Journal of Automotive Technology*. 20(5), 971–978. DOI: <https://doi.org/f9ws>
- Zsombok, I., Zöldy, M. (2023). Modelling, Simulation and Validation of Hybrid Vehicle Fuel Consumption. *Acta Polytechnica Hungarica*, 20(5). 61–74. DOI: <https://doi.org/kv2x>



# Maritime accidents affect the environment

Sara Rodriguez Martinez  
Hamburg, Germany  
Kühne Logistics University  
[sara.rodriguez@stud.the-klu.org](mailto:sara.rodriguez@stud.the-klu.org)

## Abstract

This paper highlights the effects of transport accidents on the environment, specifically those occurring in maritime transportation. International trading and shipping are important for several reasons. International trade and shipping facilitate the movement of goods and services between countries, contributing to economic growth and development. It allows countries to access resources, products, and markets they might not have domestically, thus expanding their economic potential. Not all countries possess the same resources or expertise. International trade enables countries to specialise in producing goods and services where they have a comparative advantage, leading to more efficient resource allocation and increased productivity. International trade provides consumers access to various goods and services at different prices. This enhances consumer choice and allows people to enjoy products that may not be available or affordable domestically. International trade fosters competition among businesses, driving them to innovate, improve quality, and reduce costs to stay competitive in the global marketplace. This benefits consumers through better products and lower prices. Export-oriented industries create jobs as they expand to meet global demand. These jobs often have higher wages due to the specialised skills required.

International trade generates foreign exchange earnings for a country, which can be used to pay for imports, service foreign debt, and invest in other countries. A positive balance of payments is crucial for a stable economy. Trade exposes people to different cultures by exchanging goods, services, and ideas. This fosters greater understanding and co-operation among nations. Dependence on a single industry or market can be risky. International trade allows countries to diversify economies and reduce vulnerability to economic shocks. Shipping and transportation networks required for international trade often lead to improvements in infrastructure, including ports, roads, railways, and communication systems. These improvements benefit not only trade but also local communities. Trade can facilitate the transfer of technology, know-how, and best practices between countries. This helps less developed countries to catch up and develop more quickly. While shipping contributes to global carbon emissions, it also promotes energy-efficient practices through demand for cleaner and more sustainable transport options. In summary, international trading and shipping are essential drivers of economic growth, job creation, innovation, and cultural exchange, fostering co-operation and stability between nations while promoting efficient resource utilisation and diversification. The author performed a detailed statistical analysis based on the accident database. It explains the impacts on the environment and some remedies for it.

Keywords: environmental effect, waterborne accident, waterborne transport

## 1. Introduction

The environment and transportation are two crucial and paradoxical facets of our world. The movement of people and goods depends very highly on transportation activities, which is also an important factor in social and economic development. Transportation-related activities, however, have significant environmental effects, such as habitat destruction and air and water pollution. Transportation also contributes to climate change (Mako *et al.*, 2021).

The environmental effects that transportation causes can have very damaging effects on both humans and the natural environment. For example, while greenhouse gas emissions lead to global climate change and cause more frequent and severe weather events like heat waves, an increase in Arctic temperatures, sea level rise, and other damaging effects, air pollution can result in respiratory issues, health problems, and neurological diseases. Unluckily, the ecosystem and biodiversity are being parallel destroyed.

In order to balance the advantages of transportation with preserving the natural environment and thus make transportation sustainable, several solutions have emerged. These include a variety of tactics, such as promoting environmentally friendly modes of transportation like maritime transport (Jugović, Debelić, Brdar, 2011).

We can better understand the environmental effects of transportation activities and work to develop more sustainable and environmentally responsible transportation practices by examining the relationship between transportation and the environment. This study offers solutions and analysis, keeping in mind what Berry said: “The earth is what we all have in common.” (Wendell Berry, 2018)

The idea of the transportation system acting as the growth engine is common. It is regarded as the foundation of the economic and social progress of the 20th century and serves as a conduit for people to interact with one another and access resources (Debelić, Vilke, Milanović, 2016). However, it also significantly destroys the environment and the upheaval of communities, which are frequently distributed inequitably. The structure of national economies has changed due to the simplicity with which materials and goods can be transported within and between countries, enabling connectivity on a global scale (Gudmundsson *et al.*, 2015).

The relationship between living and non-living things and their surroundings is known as their environment. The environment should be viewed as the setting for life in this sense. Remembering that people are an integral part of the environment is important. The United Nations World Charter for Nature emphasises humanity’s connection to nature (United Nations, 1982).



This paper offers a brief overview of the basic concepts used in the study of maritime accident effects, overviews accident types and offers some general solutions to the problems.



Figure 1: Birds-eye View Photo of Freight Containers

(Source: <https://www.wallpaperflare.com/birds-eye-view-photo-of-freight-containers-aerial-shot-building-wallpaper-gydai>)

## 2. What is maritime transportation?

Maritime transportation is transporting goods, people, raw materials, and semi-finished products using ships, especially on seas. This branch of transport is required to offer not only transportation-related services but also other related and wider logistical services in a more effective manner (Song, Panayides, 2015). Maritime logistics is a term that frequently refers to the maritime transport system, which is deeply interlinked with the entire logistics flow (Dvorak et al., 2020). The main benefit of maritime logistics is that it consistently achieves high operational effectiveness and customer service.



Figure 2: Container ship,  
(Source: EUROSTAT, 2023)

### 2.1 What are accidents?

Maritime transportation accidents occur while transporting goods or people by ships, boats, or watercraft. Causes may include human error, defective equipment, and unfavourable weather. Examples include fires, explosions, capsizing, sinking or grounding, resulting in fatalities, injuries and environmental harm (Li, Ren, Yang, 2023). International organisations like the International Maritime Organization have established rules and standards to ensure safety, including crew training, certification, and adherence to operational and safety standards.



## 2.2 Types of accidents

As mentioned, accidents are unexpected events that can occur during a commercial trip and can happen in many ways. According to the European Maritime Safety Agency (EMSA), a casualty occurs when one of the following conditions is met:

- “1. The death of, or serious injury to, a person;
2. The loss of a person from a ship;
3. The loss, presumed loss or abandonment of a ship;
4. Material damage to a ship;
5. The stranding or disabling of a ship or the involvement of a ship in a collision;
6. Material damage to marine infrastructure external to a ship that could seriously endanger the safety of the ship, another ship or an individual;
7. Severe damage to the environment, or the potential for severe damage to the environment, brought about by the damage of a ship or ships.” (EMSA 2022, EMSA 2023)

The following figures show how the number of maritime accidents has diminished over the previous decade (Figure 3), their ratio to total number of accidents (Figure 4) and their time series if any tendencies could be defined (Figure 5):

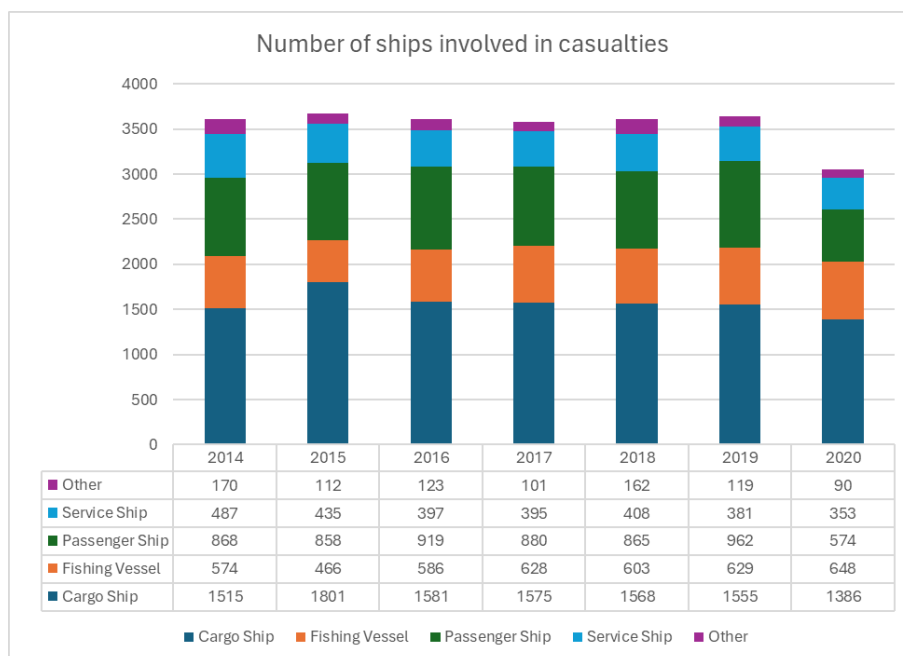
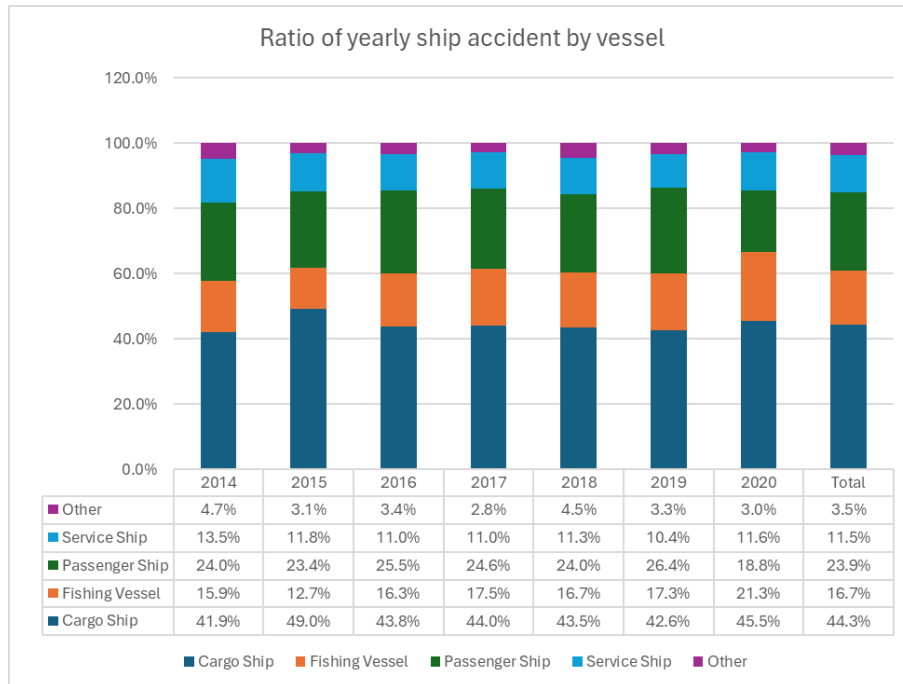


Figure 3 Numer of ships involved in accidents with casualties  
(Source: Bilogistik, 2019, Sepehri et al. 2022, EMSA, 2022, EMSA 2023)

Figure 3 offers a more comprehensive perspective that cargo ships are the ones that suffer the most casualties. The information in the table above pertains to each type of ship’s annual fatalities for 2014-2020. The author is aware that the number of accidents alone cannot describe the risk of shipping, although performance or distance-based comparison of different waterborne transport is impossible due to the lack of a coherent and transparent database.





*Figure 4 Ratio of ships involved in accidents with casualties*  
 (Source: own calculation based on Bilogistik, 2019, Sepehri et al. 2022, EMSA, 2022, EMSA 2023)

It can be seen in Figure 4 and Figure 5 that the accident share of passenger ships significantly dropped, most probably due to the COVID-SARS-19 pandemic. The cargo ship and service ship ratio is nearly constant over time. Meanwhile, the role of fishing vessels is increasing, most probably due to increasing fishing activity.

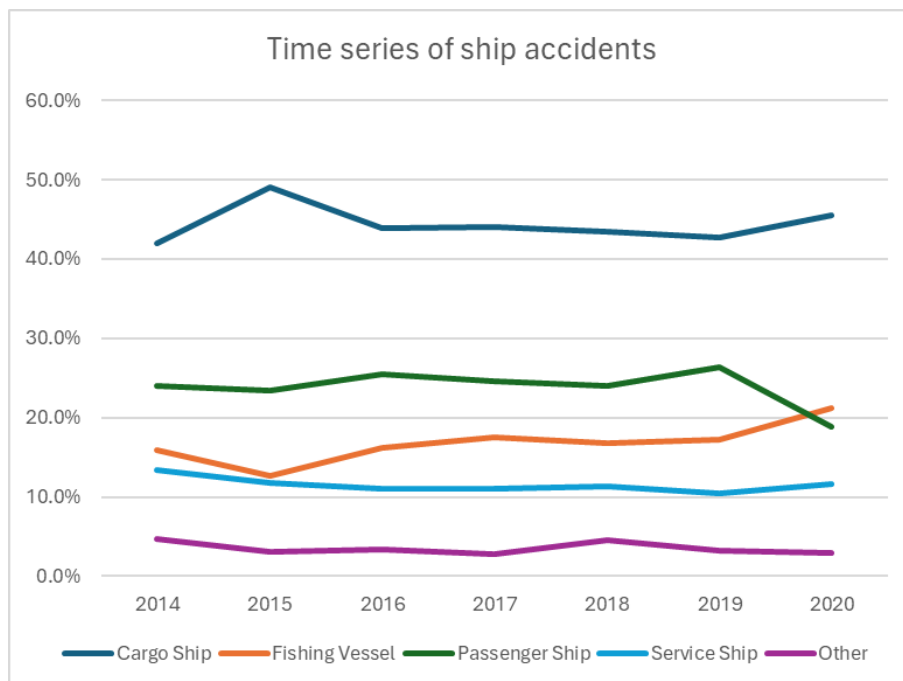


*Figure 5 Time series of ships involved in accidents with casualties*  
 (Source: own calculation based on Bilogistik, 2019, Sepehri et al. 2022, EMSA, 2022, EMSA 2023)



The average number of accidents and standard deviation of each type were calculated in this table to indicate how much variability there is in the data:

Table 1 Descriptive statistical analysis of maritime accidents 2014-2020

	Average	Standard Deviation	ST/AVG
<b>Cargo Ship</b>	1569	123	7.8%
<b>Fishing Vessel</b>	591	61	10.3%
<b>Passenger Ship</b>	847	126	14.9%
<b>Service Ship</b>	408	43	10.5%
<b>Other</b>	125	30	24.0%
<b>Total</b>	3539	218	6.2%

(Source: own calculation based on Bilogistik, 2019, Sepehri et al. 2022, EMSA, 2022, EMSA 2023)

Based on Table 1, it can be stated that although the number of other types of accidents is very low, they vary a lot over time. Meanwhile, the largest number of accidents can be connected to cargo ships, deviation of accidents are low.

### 2.3 Effects of Accidents on the Environment

There are some significant and frequently long-lasting effects that maritime mishaps can have on the environment:

1. Oil spills from ships can seriously harm the environment because the oil can cover large areas of the ocean and shorelines, causing the death of marine life and, thus, ecosystem disruption. Oil can stay in the ocean for a very long time, which makes spills have long-lasting effects on the environment.

In the figure below, there is a representation of what an oil spill causes to the marine environment. Figure 6 was chosen because oil spills have the most detrimental environmental effects.

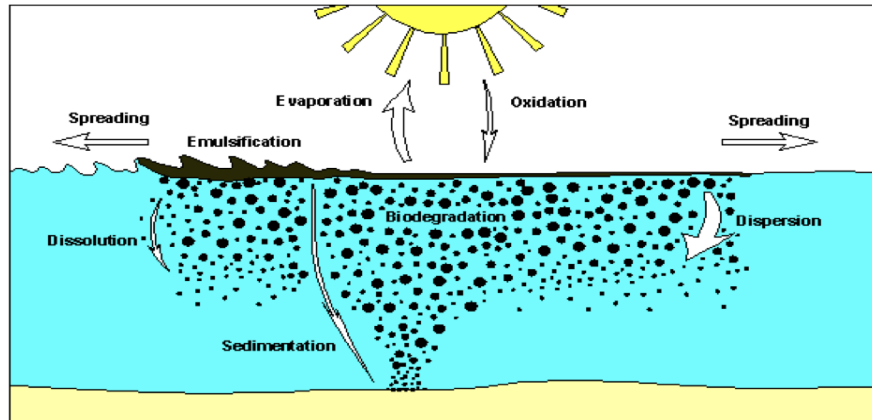


Figure 6: Fate of oil spill in the marine environment (Weathering Process),  
(Source: Kozanhan, 2019: .9)

The weathering process describes the physical and chemical changes caused by exposure to air, sunlight, water, and other natural elements. It is a process that occurs when oil leaks into the marine environment. This process can impact the outcome of the oil spill in several ways.

2. Chemical Spills: Depending on the quantity of chemicals released, ship spills can seriously harm the environment. Chemical spills can harm humans, animals, and marine life while contaminating the soil, water, and air.
3. Habitat Destroying Accidents: Maritime mishaps like collisions or groundings can physically destroy coral reefs, seagrass beds, and other crucial marine habitats. It may take years or even decades for these ecosystems to recover.
4. Noise pollution: Marine life, such as whales, dolphins, and other marine mammals, can be disturbed by ship noise, which may interfere with their ability to communicate and navigate.



5. Non-native species can be found in ballast water discharged by ships. These species compete with native species and cause ecosystem disruption.
6. Climate Change: The emission of greenhouse gases like carbon dioxide and methane during maritime transport contributes to climate change. These emissions may contribute to ocean acidification, damaging ecosystems and marine life. This, in turn, causes harm to human society.

## 2.4 Minimising the impact

Several approaches can be used to lessen the environmental harm caused by maritime accidents. The best strategy is prevention through effective safety measures, crew training, and safety protocols. A successful emergency response strategy incorporating containment booms and skimmers can be extremely important. Tougher environmental regulations, like prohibitions on ballast water discharge and requirements for low-emission fuel, can aid in minimising the impact of maritime transportation. Innovative technologies can be used to reduce greenhouse gas emissions and halt the spread of invasive species, such as alternative fuels and ballast water treatment. International co-operation is essential to address the global nature of maritime transport and its effects on the environment, including the development of global laws and standards and co-operation between nations and organisations. In the wake of an accident, restoration is crucial. Examples include removing trash, repairing damaged ecosystems, and aiding affected communities.

## 3. Conclusion

Environmental impacts of maritime transportation can be significant and widespread. Maritime transportation's main environmental effects include introducing invasive species, habitat destruction, and air and water pollution. The main source of air pollution from maritime transportation is the emission of greenhouse gases like carbon dioxide and other pollutants like sulfur and nitrogen oxides, which can negatively impact human health and the environment.

Untreated ballast water discharge, oil spills, and the release of other chemicals and waste materials into the ocean are just a few of the many sources that can lead to water pollution. These contaminants can harm marine life, destroy habitats, and contaminate human food sources. Significant environmental effects of maritime transportation include the destruction of habitat. While the movement of ships can introduce non-native species into new environments, which can have detrimental effects on local ecosystems, the construction of ports, dredging, and waste disposal are all activities that can harm coastal and marine ecosystems. In conclusion, there is a need for ongoing efforts to reduce the negative effects that maritime transportation has on the environment. The shipping industry and regulatory bodies must collaborate to develop and implement measures to reduce air and water pollution, prevent oil spills and other types of pollution, and minimise habitat destruction and the introduction of invasive species. To ensure that the environmental impacts of maritime transport are minimised while still meeting the rising demand for international trade and commerce, co-operation between governments, industry, and other stakeholders will be necessary. Additionally, digitalisation is essential to improving the sustainability of maritime transportation. The maritime sector is becoming more cost-effective, efficient, and environmentally friendly thanks to integrating new technologies and digital platforms.

## References

- Berry, W. (2018). "The earth is what we all have in common." (1 April 2018). *Marktheworld*. URL: <https://marktheworld.wixsite.com/marktheworld/post/the-earth-is-what-we-all-have-in-common.-wendell-berry> (Downloaded: 02 March 2023).
- Bilogistik, S.A. (2019). Types of ships, based on the cargo they carry. URL: <https://www.bilogistik.com/en/blog/types-ships-based-on-cargo/> (Downloaded: 26 March 2023).
- Debelić, B., Vilke, S., & Milanović, S. (2016). Port Competitiveness and Ecological Impact of Logistics Activities: A Case Study of The Port of Ploče. *Business Logistics in Modern Management*. URL <https://hrcak.srce.hr/ojs/index.php/plusm/article/view/4666>
- Dvorak, Z., Rehak, D., David, A., & Cekerevac, Z. (2020). Qualitative approach to environmental risk assessment in transport. *International Journal of Environmental Research and Public Health*, 17(15), 5494. DOI: <https://doi.org/gq8h34>
- EMSA – European Maritime Safety Agency (2022). EMSA Annual Overview of Marine Casualties and Incidents 2021. URL: <https://www.emsa.europa.eu/fc-default-view/tagged/85-annual-overview.html> (Downloaded: 10 March 2023).
- EMSA – European Maritime Safety Agency (2023). EMSA Outlook 2023. URL: <https://emsa.europa.eu/> (Downloaded: 11 April 2023).
- EUROSTAT (2023). Majority of EU freight transport in 2021 via sea. *EUROSTAT*. URL: <https://ec.europa.eu/eurostat/web/products-eurostat-news/w/DDN-20230316-2> (Downloaded: 23 July 2023).
- Gudmundsson, H., Hall, R., Marsden, G., Zietsman, J. (2015). *Sustainable Transportation: Indicators, Frameworks, and Performance Management*. Samfundslitteratur. Springer. URL: <https://link.springer.com/book/10.1007/978-3-662-46924-8>




- IMO – International Maritime Organization (n.d.). International Convention on Oil Pollution Preparedness, Response and Co-operation (OPRC). URL: [https://www.imo.org/en/About/Conventions/Pages/International-Convention-on-Oil-Pollution-Preparedness,-Response-and-Co-operation-\(OPRC\).aspx](https://www.imo.org/en/About/Conventions/Pages/International-Convention-on-Oil-Pollution-Preparedness,-Response-and-Co-operation-(OPRC).aspx) (Downloaded: 20 March 2023).
- Jugović, A., Debelić, B., & Brdar, M. (2011). Short Sea Shipping In Europe Factor Of The Sustainable Development Transport System Of Croatia. *Scientific Journal of Maritime Research*, 25(1). pp109-124 URL: <https://hrcak.srce.hr/clanak/103833>
- Keltic Petrochemicals Inc. (2007). Effects on the environment, URL: [https://iaac-aeic.gc.ca/archives/evaluations/10471/documents\\_staticpost/pdfs/23818-10E.pdf](https://iaac-aeic.gc.ca/archives/evaluations/10471/documents_staticpost/pdfs/23818-10E.pdf) (Downloaded: 20 March 2023).
- Kozanhan, M. K. (2019). Maritime Tanker Accidents and Their Impact on Marine Environment. *Scientific Bulletin of Naval Academy*. 22(1), 1–20. DOI: <https://doi.org/knt2>
- Li, H., Ren, X., Yang, Z. (2023). Data-driven Bayesian network for risk analysis of global maritime accidents. *Reliability Engineering & System Safety*. 230, 108938. DOI: <https://doi.org/kntx>
- Mako, P., Dávid, A., Böhm, P., & Savu, S. (2021). Sustainable transport in the Danube region. *Sustainability*, 13(12), 6797. DOI: <https://doi.org/kntw>
- Sepethri, A., Vandchali, H. R., Siddiqui, A. W., Montewka, J. (2022). The impact of shipping 4.0 on controlling shipping accidents? A systematic literature review. *Ocean Engineering*. 243, 110162. DOI: <https://doi.org/kntz>
- Song, D. W., Panayides, P. (2015). *Maritime Logistics: A Guide to Contemporary Shipping and Port Management*. Kogan Page. p446. ISBN: 9780749472689
- United Nations (1982). World Charter for Nature. URL: <https://digitallibrary.un.org/record/39295>



# Environmental Capacity Through the Moral Economic Lens – Dynamic Equilibria

Zsófia Hajnal

 0000-0001-8089-9930

Corvinus University of Budapest,  
Budapest, Hungary  
zsofia.hajnal@stud.uni-corvinus.hu

## Abstract

This article explores and maps hierarchical, dynamic environmental-economic equilibria. Based on the moral economic premise of finite human needs, on output that increases with the population number in a supralinear manner, and on technology levels, moral economic equilibria are identified and quantified. These equilibria are compared to environmental capacities – as a function of technology levels. A needs-based, theoretical attempt is made to resolve the tensions and conversion issues in the economic-environmental nexus. A novel, visual, moral, and economic model of equilibria with the environment is established and justified. The model is expected to suggest indirect economic adjustments to align with sustainability, which is more of a notion to be aligned with constantly than a handful of one-time economic targets to meet.

## Keywords

moral economics, environmental capacity, technology, human needs, equilibrium

## 1. Introduction

Groups and networks of economists, economic advisors and decision-makers face global economic-environmental calibration challenges. Beyond the – many times literal – firefighting, they bare a responsibility for figuring out how life for future generations could be safer, free, and sustainable. This paper does not discuss recent phenomena of climate extremes around the world, albeit they are heavy reminders of our species' environmental overexploitation. Rather, it focuses on the general and long-term economic-environmental relationships. Establishing these theoretical connections is long overdue, for “there is an urgent need for more rapid integration of economics into the core of sustainable development, and more rapid integration of sustainable development into the core of economics” (*Polasky et al., 2019, p. 5234*). The largely visual model in this paper may lie at the heart of the integration on both sides.

### 1.1. Theoretical background

The paper's title calls for two initial concept introductions and clarifications: those of moral economics and those of environmental capacity.

*Moral economics* is a branch that can potentially incorporate ethical elements into economic theories or models. It is relatable to, but not to be identified or confused with, the “moral economy” tradition. It is one of the pluralistic economic expressions – humane economics and the social and solidarity economy – aiming to expand economic knowledge and well-being in tandem. In the author's interpretation, moral economics expands economic understanding in three major directions: incorporating ethical factors into economic models, expanding the economic understanding of the environment, and re-axiomatizing human needs. This research will borrow tools from the latter two directions. Hungarian scholars whom the author would categorize as advocates of moral economics include Balázs Hámori (from a behavioural economic viewpoint), Laura Baritz (from a religious perspective), Gergely Tóth (advancing the environmental aspects), and László Zsolnai (representing the ethical direction). Internationally, the author regards Amitai Etzioni, Samuel Bowles, and Mariana Mazzucato, among others, as key figures in advancing and popularising moral economics through experimenting with ethical-economic interactions, both in theory and practice.



*Environmental capacity*, “the maximum population size an environment can sustain indefinitely” (Australian Academy of Science, n. d.), also called carrying capacity, is. Extraterrestrial space is included in this concept, interpreted as part of our environment. There appears to be a gap in the economic-environmental discourse in this area. Environmentally, in the short and mid-term (for the next few decades), humankind is in a “firefighting” mode, with incentives and attempts to restrict material production and consumption – growth, in general. The conversion between the economic and the environmental, however, is incomplete (Bartus, 2008, p. 1021), leaving theoretical space for increasing value-creation – both private and collective (Mazzucato, 2022, p. 8), and practical space as well, on the long term.

In finding economic-environmental equilibria, human needs play a decisive role. Like the environment, converting human needs into economically expressed units is incomplete. However, human needs are directly relatable to environmental ones. The author presumes that constructing a system of models which incorporates all three areas (human needs, the economy, and the environment) allows for a clearer overview of equilibria. This system will require the moral, economic axiom of finite needs, i.e. human needs being satiable, ultimately and sustainably.

## 1.2. Research questions and methodology

The paper's research questions are: What are the determinants of environmental-economic equilibria in the moral-economic sense? What are the moral and economic criteria for “sustaining sustainability” regarding economic relations? What are the practical and future implications of the findings?

In order to answer these questions, the system mentioned above of models is outlined, illustrating how the altered axioms of finite needs and cooperation have far-reaching implications for the global economy. The analysis is conducted in the context of the relevant literature. Data from the World Bank is used to determine the system’s rightfulness. Due to its novelty and scope, however, the system of models will be presented as a simplified construct – it is rather opening doors for further research and adjustments than applicable straightaway.

## 2. Outline of the visual model

In order to make the system that is built comprehensible, the article will introduce the concepts used and premises applied gradually. The first two subchapters rely on the book *Moral Economics – A Theoretical Basis for Building the Next Economic System* (Hajnal, 2021, pp. 76–78).

The following relationships will be dealt with:

- human needs as a function of the population number;
- output as a function of the population number;
- the intersections of needs and output;
- the intersections of needs and output at different levels of technology;
- the intersections of needs and output as a function of the level of technology, limited by the environmental capacity.

Human needs, the population number, and the level of technology are seen as exogenous factors.

### 2.1. The aggregate of finite human needs

As mentioned, the “finite and satiable” premise applies to human needs. Human needs display a dynamic and wide variety of types and intensities, constantly changing in time for each individual. Traditionally, they are not measured in their aggregate due to the resulting lack of an unit of measure (UOM) and the aforementioned incomplete conversion between human needs and economic ones. This research, however, attempts to measure and illustrate the needs to combine the concepts. Units are used flexibly, referring both to economic value (utils, satisfiers) and to forms of energy.

When needs are seen as finite with respect to the individual, the needs-aggregate for a given number of people also yields a distinct value. Thus, the aggregate function of needs in the *population number – value or energy* coordinate system is an upward sloping, linear one, as depicted in *Figure 1*.

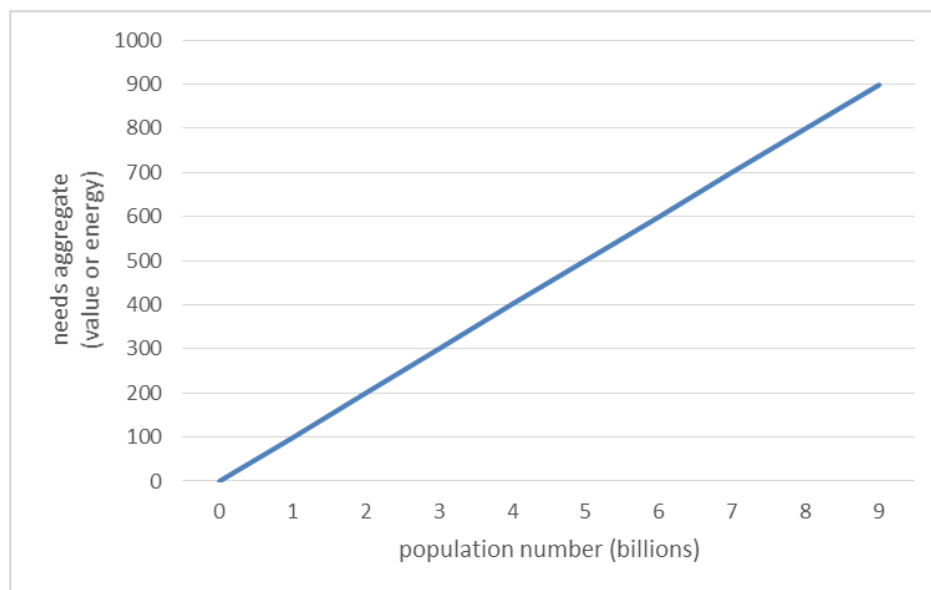


Figure 1: The needs-aggregate as a function of the population number. Generated by the author.

## 2.2. Output as a function of the population number

When depicting potential output, the paper operates with a more general notion than traditionally used in macroeconomics. Moreover, in this socio-optimistic approach, it will be presumed that output always increases with the population number increasing, in a supralinear manner. This approach relies on labour division and the increasing opportunities for cooperation, by incorporating the efficiency-increasing effects of these phenomena. In this form, output, as a function of the population number, resembles an exponential function, as depicted in *Figure 2*, with curve *1a*. With slightly more skepticism, pessimism, or simply a more critical attitude, taking challenges to cooperation into account, potential output in the “population number – value or energy” coordinate system can be depicted as an S-shaped curve (*Figure 2*, curve *2a*). The inflection point illustrates how the effects of cooperation become strengthened (through technology), but then, the given technology level is not yet suitable for facilitating an even larger-scale of cooperation.

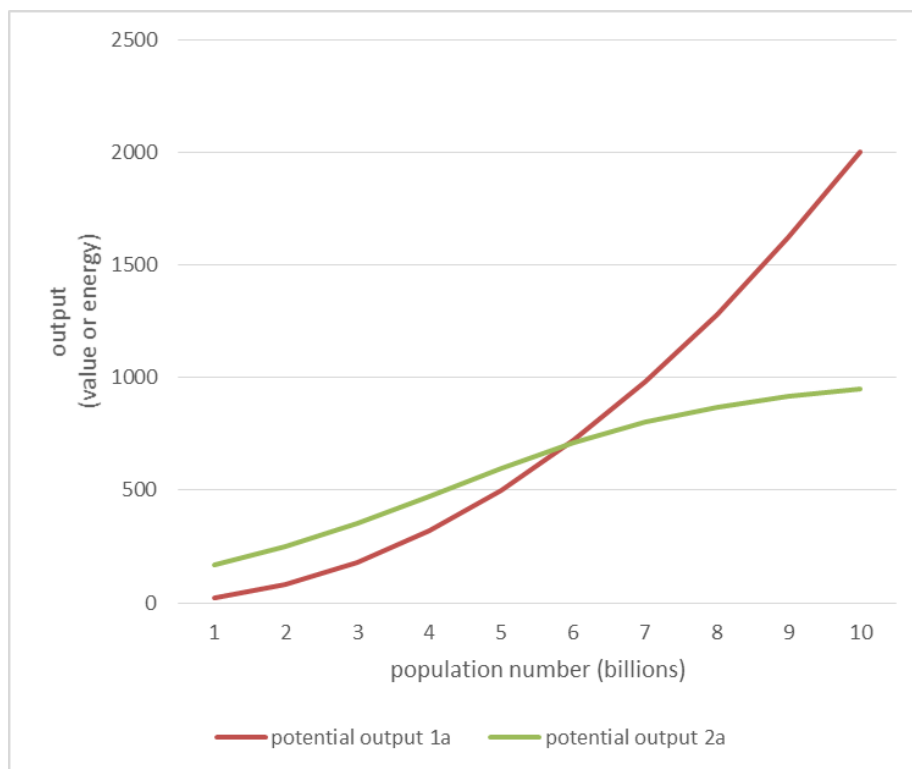


Figure 2: Two scenarios for (potential) output as a function of the population number – socio-optimistic (exponential) vs. critical (S-shaped) approaches. Generated by the author.

### 2.3. The intersections of needs and output

Combined in one system, as done in *Figure 3*, the needs aggregate and potential output have one or two intersections, depending on the shape of the functions at the given level of technology (whether potential output is seen as exponential or as an S-shaped function).



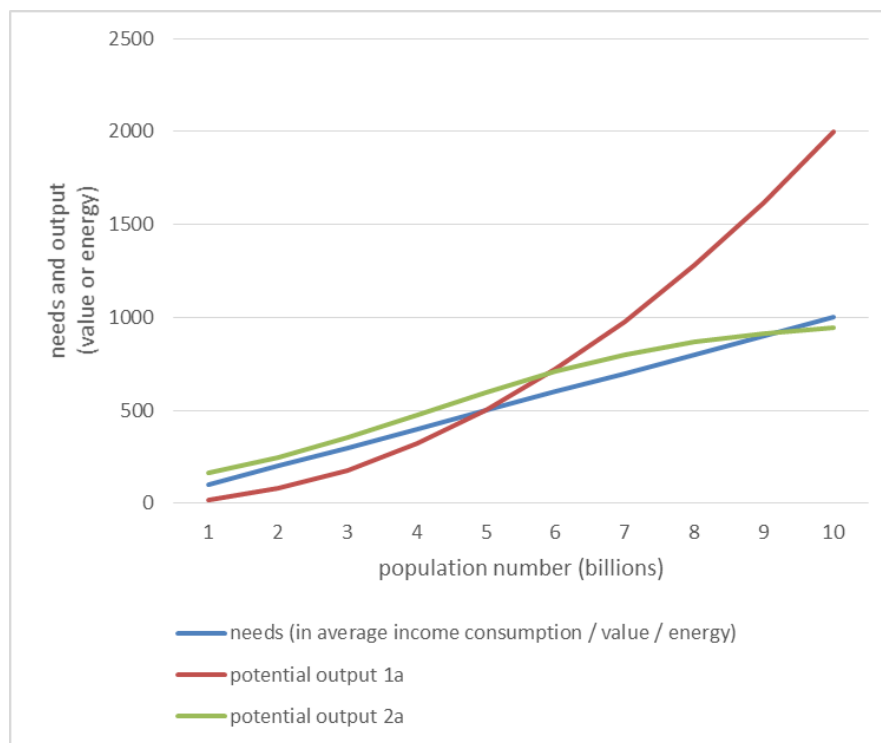


Figure 3: Intersection variations of the needs aggregate and the output function.  
Generated by the author.

An S-shaped output function with two intersections implies three key phases on the given function:

- First, where the population number is relatively small, and output is below the needs, the population experiences scarcity.
- Second, where the population number is greater, and output crosses over to be more abundant, the problem of unemployment may arise.
- Third, beyond the inflection point and the second intersection of the S-shaped output with needs, output is scarce again. This, however, may be a more stable area of the coordinate system: despite the scarcities, the larger population number is a greater guarantee for non-extinction.

#### 2.4. The intersections of needs and output at different levels of technology

The level of technology is traditionally not accurately measurable on a macro-scale, for some of its characteristics (unit of measure, maximum value) are undefined (*Hajnal, 2022, p. 10*). However, the interpretations thus far in the paper – of the output level and its intersection with the needs-aggregate – are interpreted in a temporal-technological context: at a given level of technology.

This paper operates with roughly constantly increasing technology levels in time. As technology progresses, the output draws closer to the Y axis (the “value or energy” axis), but aggregate human needs do not. These notions – the linear function of finite needs, and the exponential or S-shaped curves of potential output at increasing levels of technology – are illustrated below, in *Figure 4*.

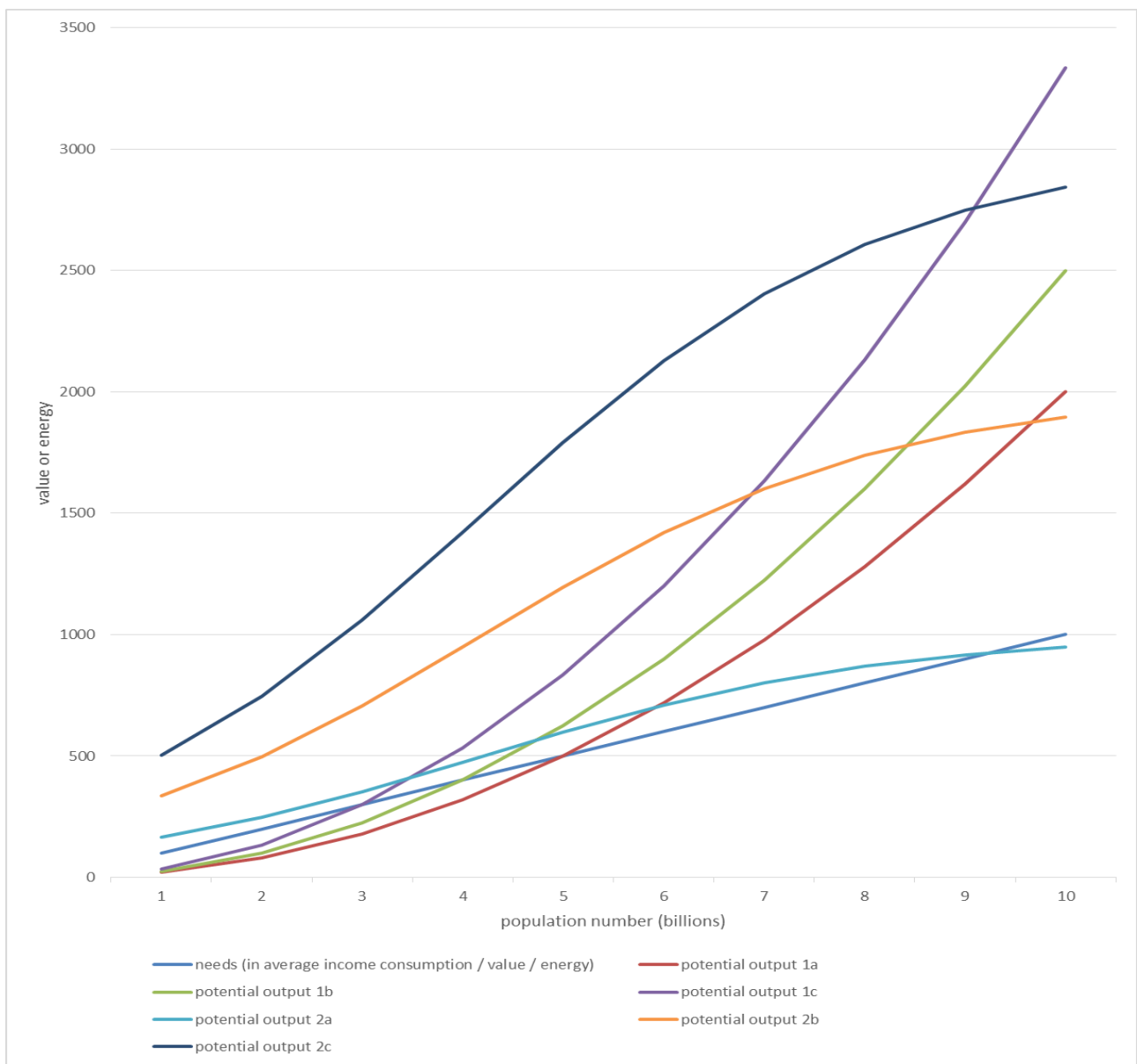


Figure 4: Intersections of the aggregate of needs and potential output, as a function of the population number. Different levels of technology are denoted by the letters a, b and c in the indices. Generated by the author.

## 2.5. The dynamic equilibria in the environmental context

This subchapter provides the theoretical synthesis of technology levels, needs-output intersections, and the environmental capacity.

The way environmental capacity comes into the picture is as follows. Moral economics views needs, thus, consumption, and thus the demand on environmental resources too, as finite. Would human needs and the level of technology be quantified, the debates of estimations around environmental capacity could be mitigated.

Changes in the level of technology affect the environmental capacity (the sustainable population number) mostly positively, but the capacity can fluctuate (as a function of the level of technology), due to damaging uses of technology, which may lead to the overexploitation of nature by humans (*Figure 5*).

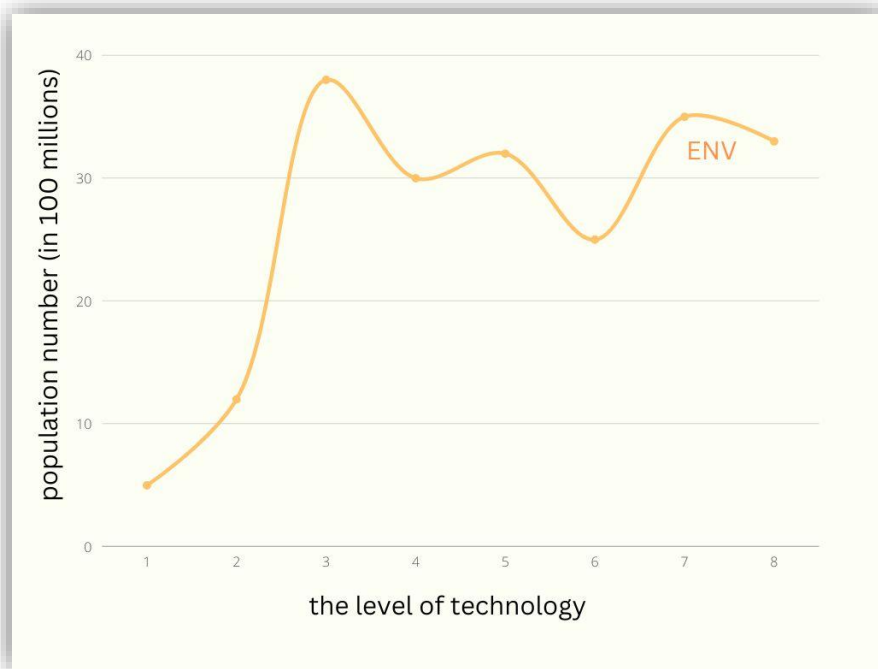


Figure 5: Environmental capacity to “carry” humans, as a function of the level of technology.  
Created by the author.

The needs-output intersections, as equilibria, are one condition of economic balance. In the broader view, the intersection(s) of needs and potential output have to be at a population number on – or more preferably – below the environmental capacity boundary (curve).

The last illustration, *Figure 6*, displays population numbers as a function of the levels of technology. The four curves are:

- EXP.: the population numbers at the intersections of needs and potential output (exponential version) at the given level of technology;
- $S_1$ : the population numbers at the first intersection of needs and potential output (if the latter is an S-shaped curve) at the given level of technology;
- $S_2$ : the population numbers at the second intersection of needs and potential output (if the latter is an S-shaped curve) at the given level of technology;
- ENV.: the environmental capacity (in terms of the population number) at the given level of technology (as depicted in *Figure 5* as well).

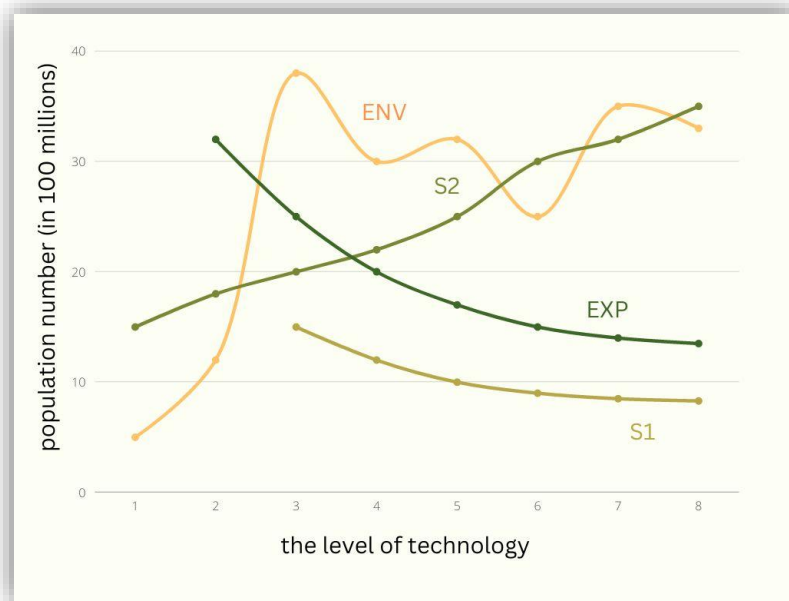


Figure 6: Population numbers at the intersections of needs and output as a function of the level of technology, limited by the environmental capacity. Created by the author.

There are environmentally stable and unstable phases over technology level changes. When the population numbers given by needs-output intersections move below the environmental capacity, humankind can be said to be environmentally safe, on the aggregate. This varies with which needs-output intersection function we look at – the one resulting from exponential output curves, or those stemming from S-shaped ones. The curves denoted with EXP and  $S_1$  represent economic equilibria mostly below the environmental limitations, yet these equilibria stem from decreasing population numbers, as a function of technology. They illustrate the fear of labour, or of human inputs becoming unnecessary.  $S_2$  represents a sequence of economic equilibria, where the population number remains large enough for probable survival, despite balancing around environmental limits at subsequent levels of technology.

Environmental capacity has increased for much of human history, starting to change with the second industrial revolution. The “troughs” on the environmental capacity curve (ENV) illustrate the overexploitation of nature.

A stable state may be hoped for in the distant future, for technologies, when applied properly, make humankind more self-reliant, less exploitative, and increase environmental capacity. Once it becomes economically and politically profitable to completely transition to renewables, harnessing those resources ought to have the aforementioned, desired effects.

To contrast the techno-optimism in the paragraph above, one could argue that technology will not save us fast enough from a complete environmental disaster – but that is not what was stated. The level of technology changes at various speeds over time, so its axis does not represent time in an absolute manner. There were only relations and mechanisms sketched. Without proper environmental and economic policies, the real population number may rise so much above both the environmental limit and the needs-output equilibrium, that it causes an irreversible environmental disaster. This latter view reflects the economic pessimism in theory.

### 3. A potential paradox

There is an economic-evolutionary paradox, relatable to the system outlined above. Nature initially nurtured our species to compete (law of the jungle). Having overcome that phase through cooperation, we have surpassed other species in several aspects. The scale of division of labour, particularly in the industrial beginnings, was yet another level of effectiveness (between competitive communities, competitive nations). Meanwhile, the competitiveness of an economic system appeared to have become dependent on its internal levels of competition. In the end, we have become so effective at production and consumption, that now, we can compete with time itself, to stay within our environmental limits.



#### 4. A quantitative illustration

From the system outlined, there are factors that can be quantified, and there are some that cannot. The latter type (currently unquantifiable factors) includes primarily the level of technology, certain types of human needs (as part of the aggregate), but there is debate around the environmental capacity as well. As for the latter: “The range of estimates is enormous, fluctuating from 500 million people to more than one trillion. Scientists disagree not only on the final number, but more importantly about the best and most accurate way of determining that number—hence the huge variability” (*Australian Academy of Science, n. d.*).

In the discussion below, concrete measures for needs and output are discussed. Figures for the year 2021 will be used to illustrate findings.

For the record, population number in this year exceeded 7.84 billion (*The World Bank, 2022c*). Economic needs can be approximated with final consumption expenditure data (for energy, food, and other products and services). The monetary (value) expression is wider than that in energy, thus the monetary expression is applied. By definition: “Final consumption expenditure consists of expenditure incurred by resident institutional units (Households, NPISHs, sector of general government) on goods or services that are used for the direct satisfaction of individual needs or wants or the collective needs of members of the community” (*Insee, 2021*). Final consumption expenditure in 2021, globally, exceeded 62.03 trillion, in current USD (*The World Bank, 2022a*). The production, or output (or supply) side is also expressed through a monetary term: Global GDP in the same year was around 96.1 trillion, in current USD (*The World Bank, 2022b*). In terms of moral economic equilibria, this may be interpreted as a point of abundance in the population number – value coordinate system.

The drawbacks of this economic arrangement are detectable in the fact that the Earth Overshoot Day, i.e. “the date when humanity’s demand for ecological resources and services in a given year exceeds what Earth can regenerate in that year” (*Earth Overshoot Day, 2022*) steadily draws closer to the beginning of the year, with the date falling on the 29<sup>th</sup> of July in 2021 (*Willige, 2022*).

These rough numbers for 2021 confirm what we already know: humankind (beyond partially overconsuming) overproduces, and that despite the global overall economic abundance, we are in an environmental “trough”.

#### 5. Practical and future implications

Solutions to the economic-environmental imbalance do not have to be restricted to or to start with the macro-factors (such as the population number) of the model outlined earlier. Environmental-economic consciousness should start with an exact mapping and quantification of human needs, before moving on to operate with the population number. Technology levels would also need to be quantified at the macro level. The model is a starting point for moral economic – environmental orientation.

Once there is a possibility for approximate (or even exact) quantifications, the moral economic approach to needs and output may theoretically enable the mathematical description of more of the various economic systems’ benefits, implying distinct levels of technology and abundance where, in terms of progress, it may be beneficial to shift from one system to another, with special regard to market vs. state powers.

Last, but not least, it should be stated that physical (environmental, or planetary) boundaries may contribute to the short/mid-term arguments for holding economic growth at bay. (See, for instance: *Rockström et al., 2009.*; *Steffen et al., 2015*; *O’Neill et al., 2018*) On the longer term, however, finite needs may be used in a more suitable and convincing reasoning. The rightfulness of this statement still depends on whether it is environmental or ecosystem services (as in: *Costanza et al., 2014*), or human needs that will be better quantifiable, better convertible into economic units and forces.

#### 6. Conclusion

The article has dealt with the environmental-economic imbalances on a macro-scale, in simplified terms, which nevertheless resulted in complex models, with dynamic equilibria. Starting from the moral economic premises of finite needs and effective cooperation, the following factors have been identified as determinants of moral economic equilibria: human needs, potential output, the population number, the level of technology, and environmental capacity.



The condition for sustainability was for the *human needs aggregate – potential output* intersections (as interpreted in the *population number – value/energy* coordinate system) to remain below the environmental boundaries in terms of the population number, in the *level of technology – population number* coordinate system.

The article has refrained from being “to the ground” in terms of principles and guidelines for moral economic sustainability, as the system of models sketched allows for space, in this context. However, the quantification requirement of needs and technology levels has been emphasized, and the models’ potential to suggest systemic shifts in economic policy has been foreshadowed.

Despite not giving a direct solution to the conversion problem in the economic-environmental nexus, the paper suggested operating with human needs as a “workaround”, which – in the opinion of the author – have a greater likelihood to be mapped and expressed economically in the future.

## References

- Australian Academy of Science. (n. d.). *How many people can Earth actually support?* URL: <https://www.science.org.au/curious/earth-environment/how-many-people-can-earth-actually-support> accessed: September 21, 2022
- Bartus, G. (2008). Van-e a gazdasági tevékenységeknek termodinamikai korlátja? [Is there a thermodynamic constraint on economic activity?]. *Közgazdasági Szemle*, 55, 1010–1022. URL: <http://epa.oszk.hu/00000/00017/00153/pdf/05.pdf> accessed: September 14, 2022
- Costanza, R., de Groot, R., Sutton, P., van der Ploeg, S., Anderson, S. J., Kubiszewski, I., Farber, S., Turner, R. K. (2014). Changes in the global value of ecosystem services. *Global Environmental Change*, 26(26), 152–158. DOI: <https://doi.org/f577jk> accessed: September 15, 2022
- Earth Overshoot Day (2022). *About Earth Overshoot Day*. URL: <https://www.overshootday.org/about-earth-overshoot-day/> accessed: September 15, 2022
- Hajnal, Z. (2021). *Moral Economics – A Theoretical Basis for Building the Next Economic System*. In: Róna, P., Zsolnai, L., Wincewicz-Price, A. (eds) *Words, Objects and Events in Economics*. Virtues and Economics, vol 6. Springer, Cham. DOI: <https://doi.org/jk54>
- Hajnal, Z. (2022). Measuring the Level of Technology in Moral Economics. *Athens Journal of Technology & Engineering* 9(4), 321–338. DOI: <https://doi.org/kjxi>
- Insee – Institut national de la statistique et de études économiques. (2021). *Final consumption expenditure – definition*. URL: <https://www.insee.fr/en/metadonnees/definition/c2216#> accessed: September 22, 2022
- Mazzucato, M. (2022). Collective value creation: a new approach to stakeholder value. *International Review of Applied Economics*. DOI: <https://doi.org/kjxh> accessed: July 15, 2023
- O’Neill, D.W., Fanning, A.L., Lamb, W.F., Steinberger, J. K. (2018) A good life for all within planetary boundaries. *Nature Sustainability* 1, 88–95. DOI: <https://doi.org/cj8t> accessed: July 15, 2023
- Polasky, S., et al. (2019). Role of economics in analyzing the environment and sustainable development. *PNAS*, 116(12), 5233–5238. DOI: <https://doi.org/gfz7fc> accessed: September 21, 2022
- Rockström, J., et al. (2009). Planetary boundaries: Exploring the safe operating space for humanity. *Ecology and Society*, 14(2), 32. URL: <https://www.ecologyandsociety.org/vol14/iss2/art32/> accessed: September 15, 2022
- Steffen, W.; Richardson, K.; Rockström, J.; Cornell, S. E.; Fetzer, I.; Bennett, E. M. . . . Sörlin, S. (2015). Planetary boundaries: Guiding human development on a changing planet. *Science*, 347(6223). DOI: <https://doi.org/f3m6n9> accessed: July 15, 2023
- The World Bank. (2022a). *Final consumption expenditure (current US\$)*. URL: <https://data.worldbank.org/indicator/NE.CON.TOTL.CD> accessed: September 15, 2022
- The World Bank. (2022b). *GDP (current US\$)*. URL: <https://data.worldbank.org/indicator/NY.GDP.MKTP.CD> accessed: September 15, 2022
- The World Bank. (2022c). *Population, total*. URL: <https://data.worldbank.org/indicator/SP.POP.TOTL> accessed: September 22, 2022



Willige, A. (2022). Earth Overshoot Day. What is it and why do we need it? *The World Economic Forum*.  
<https://www.weforum.org/agenda/2022/06/earth-overshoot-day-human-consumption-biicapacity-ecological-footprint/> accessed: September 15, 2022



# Application of mathematical models to Euro Standard passenger car curves for predicting the future of the market

Ignacio DURÁ IBORRA  
Universitat Politècnica de València  
Valencia, Spain  
[idoribo@etsii.upv.es](mailto:idoribo@etsii.upv.es)

## Abstract

In Europe, vehicle emissions are regulated by the Euro Standard legislation. Governments of different countries force automotive industries to adapt their vehicles to comply with these standards. The legislation is regularly updated to reduce vehicle emissions and control the issue of gas emissions. This study aims to examine previous regulations and adapt three different mathematical models to their market curves. The information collected proposes three possible predictions for the future Euro Standard. This will aid the anticipation of future regulations and enable adaptation to the demands of the future market of passenger cars.

## Keywords

Euro Standard, mathematical model, prediction

## 1. Introduction

Predicting the future market penetration of passenger cars is crucial for several reasons:

- **Business planning:** Automakers, suppliers, and related industries must make strategic decisions regarding production, capacity, and investments. Accurate predictions of market penetration help them allocate resources effectively, optimise production levels, and plan for potential shifts in demand.
- **Financial performance:** Accurate market penetration predictions can impact the financial performance of companies. How well companies anticipate market trends and adapt their strategies can affect stock prices and investor confidence.
- **Technology development:** The automotive industry is rapidly evolving, with advancements in electric vehicles (EVs), autonomous driving, connectivity, and alternative fuel technologies. Predicting market penetration helps companies align their research and development efforts with future demand for these technologies.
- **Policy and regulations:** Governments and regulatory bodies use market penetration projections to design policies, incentives, and regulations that encourage the adoption of cleaner and more efficient vehicles. Accurate predictions can help set realistic targets for emissions reduction and sustainable transportation goals.
- **Environmental impact:** The transportation sector significantly contributes to greenhouse gas emissions and air pollution. Predicting future market penetration of electric and other eco-friendly vehicles helps assess the potential environmental impact and plan for a more sustainable future.
- **Infrastructure planning:** Adopting new vehicle technologies requires infrastructure development, such as charging stations for EVs or hydrogen refuelling stations for fuel cell vehicles. Predictions help stakeholders plan and invest in the necessary infrastructure to support changing market needs.
- **Consumer behaviour:** Understanding future market penetration helps automakers anticipate consumer preferences and demands. This insight allows them to tailor their marketing strategies, product offerings, and pricing to meet customer expectations.
- **Competitor analysis:** Market penetration predictions provide valuable information for competitive analysis. Companies can gauge their market share and understand how their competitors may respond to changing market dynamics.

Predicting the future market penetration of passenger cars is essential for making informed decisions, staying competitive, promoting sustainable growth, and contributing to a more environmentally friendly transportation system.

Currently, the latest standard in force is Euro Standard 6d. However, the study will focus on the Euro 3, Euro 4, Euro 5 and Euro 6 Standards to have a transparent and robust analysis. Their limits are the acceptable amount of exhaust gases to be used as a solid basis for upper estimation. Regulated emissions include carbon monoxide (CO), hydrocarbons (HC), nitrogen oxides (NO<sub>x</sub>) and particulate matter (PM). Some of these pollutants contribute to the greenhouse effect, while others harm human health by causing respiratory and other problems (*Bereczky and Török, 2011*). The limits are measured as an emitted gram of pollutant per kilometre driven (*Tánczos and Török, 2008*). There is no fixed period, but from time to time, the regulations are revised, and the limits are tightened according to scientific evidence and environmental goals (*Figure 1*). The regulations are adapted to the type of vehicle, distinguishing between petrol and diesel-powered vehicles:



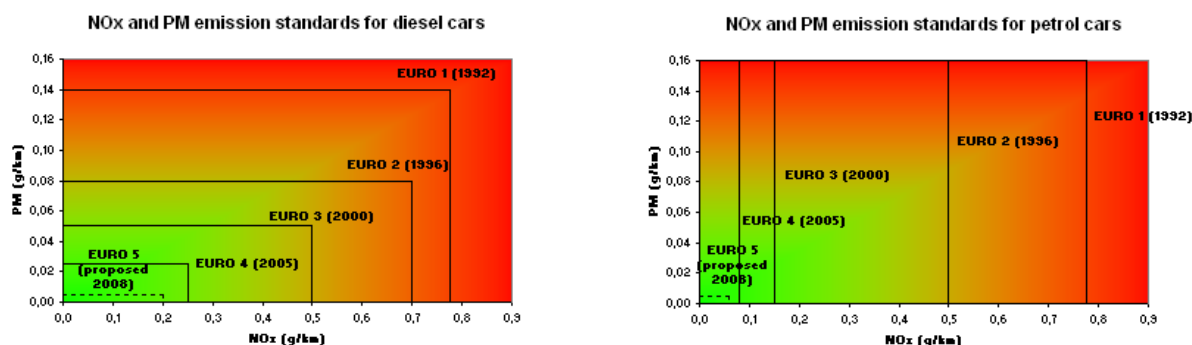


Figure 1: EURO emission reduction development example for NO<sub>x</sub> and PM  
(source: Academic Dictionaries and Encyclopedias)

The following investigation aims to study the registration curves of passenger cars that meet the vehicle emission standards set by the Euro Standard legislation using the Microsoft Excel Solver tool. The idea is to approach three different mathematical models to the previous Standard curves, collect information and, with this forecast (Lekić et al., 2021), the possible future Euro Standard 7 curve. The models selected have been: the Logistics Model, Gompertz Model and Gaussian probability distribution (Für and Csete, 2010).

## 2. The mathematical model

The models that will be used are the Logistic model, the Gompertz model and the probabilistic Gaussian distribution. The first two models are used in contexts of exponential population growth. At the same time, the latter model describes natural and human phenomena that tend to group around a central value or are symmetrical. While it is true that the case study is far from being a setting in which these models are typically used, the passenger car sales market can be assumed to be an analogy for population growth.

### 2.1 The logistic model

The logistic population growth model is a differential equation that describes the growth of a population as a function of time (Radpour et al., 2021). It is used when a population grows exponentially initially, but as it approaches the maximum carrying capacity of the environment, growth slows and eventually stabilises. The equation is as shown in (1):

$$N(t) = \frac{N_0 \cdot K}{N_0 + (K - N_0) \cdot e^{-rt}} \quad (1)$$

Where

- $N(t)$  is the population at time  $t$  ;
- $N_0$  is the population at the initial time ;
- $K$  is the maximum capacity of the population or the carrying capacity ;
- $r$  is the population growth rate.

### 2.2 Gompertz model

The Gompertz Model is a function used in various fields, such as biology or automobile market analysis (Rota et al., 2016). It is often used to model the growth of organisms or cells. The function has the formula shown in (2):



$$f(t) = a \cdot e^{-be^{-ct}} \quad (2)$$

Where

$f(t)$  is the value of the function at time  $t$ ;  
 $a$  represents the maximum asymptotic value that can be reached ;  
 $b$  is related to the initial growth rate, a higher  $b$  indicates faster growth at the beginning;  
 $c$  is associated with the decrease in growth rate as the population reaches the maximum limit. A higher value indicates a faster decline in growth rate.

### 2.3 Gaussian model

The Gaussian or normal probability distribution is one of the most widely used statistical distributions and describes a bell-shaped curve (*Wang et al., 2022*). Its equation is shown in (3):

$$f(t) = a \cdot e^{(-b \cdot (x-c)^2)} \quad (3)$$

Where

$f(t)$  is the value of the function at the point  $t$ ;  
 $a$  is the amplitude, a constant which affects the height of the bell;  
 $b$  is a parameter that determines how fast the bell falls;  
 $c$  is the central value of the bell, and it is known as the mean-

### 2.4 Excel Solver Tool

The tool used to achieve the analysis was Excel Solver. This tool has different functions. Among them, it allows the Excel environment to modify the value of a cell dependent on other cells by modifying the value of these other cells. The analysis will provide passenger car (PC) sales year by year for each Euro Standard. Subsequently, it will approximate each mathematical model to the real sales curves. It will minimise the cell containing the sum of the squared errors between reality and the mathematical models by modifying the values of the parameters of the mathematical models. The errors are quadratic to avoid cancellation between positive and negative values. Most smaller players will likely either be bought or merged with other big players. As the industry matures, cost efficiency will play a more significant and prominent role. If a smaller actor wants to stay independent, he must specialise.

## 3. Results

This section will present the Euro curves of standards 3, 4, 5, and 6. Thanks to the European vehicle market statistics pocketbook, the percentage of registered passenger cars (PC) that meet the different Euro Standards can be obtained, see (*Figure 2*):

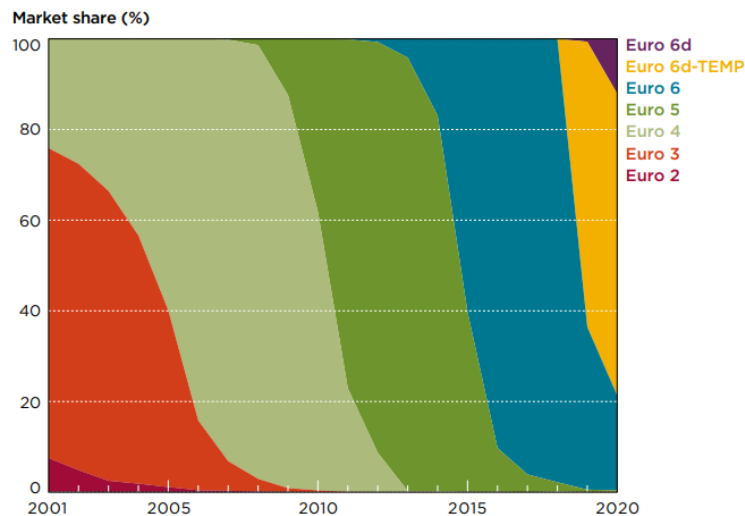


Figure 2. Percentage of new PC registrations  
 Source: *European Vehicle Market Statistics Pocketbook 2021–2022 p50*

Besides, the amount of newly registered passenger cars (PC) is known (Figure 2). With these sources of information, the number of newly registered PC which accomplishes the different Euro Standards can be obtained and represented (Figure 3):

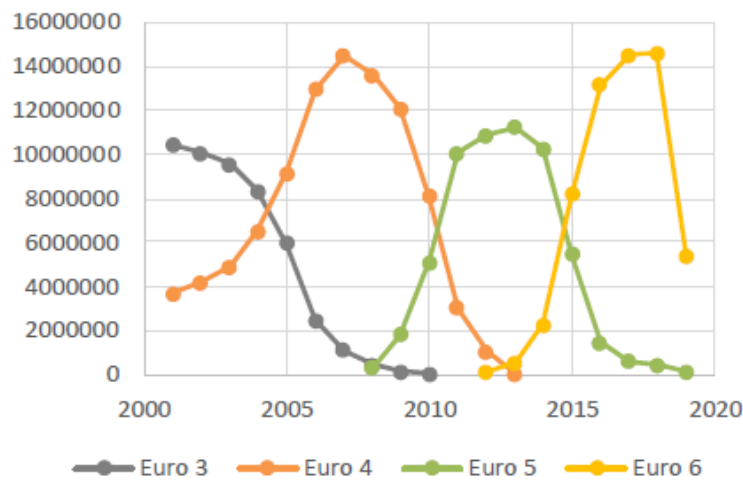


Figure 3. Euro Standard PC registrations curves  
 Source: *own edition based on European vehicle market statistics pocketbook 2021–2022 and ACEA 2022*

In this section, the approximation of the mathematical models to the curves will be presented. Only the approximation of the Logistic Model will be presented to avoid repetition. However, the process followed is analogous to the rest of the models. At first, it may not seem possible to approximate the mathematical model to one of these curves. However, with a couple of changes, this is straightforward. First, the curves will be divided into two at the midpoint. The first half of the bell resembles the Logistic Model, so the approximation is straightforward. The procedure for the second bell requires a reverse ordering of the data so that the curve is similar to Logistic Model. Once the approximation is made, the approximated data will be rearranged according to the initial pre-arrangement scheme to maintain the bell shape. Since the central value of the bell is used in both approximations, the mean of the approximations will be taken as the final value. Figure 4 presents the Logistics Model's final results.

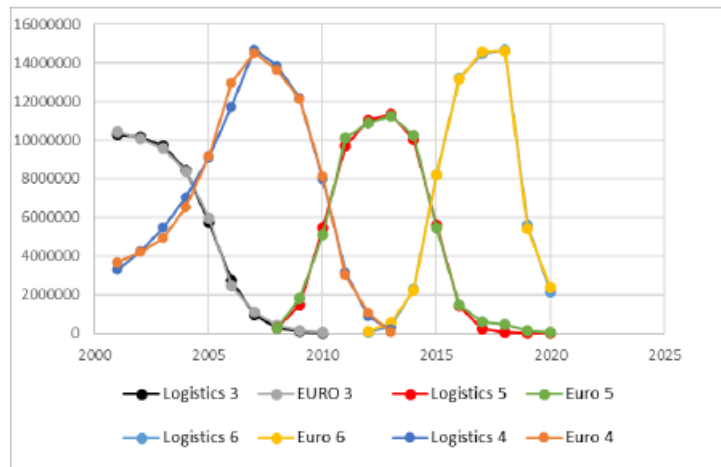


Figure 4. Logistics Model approximations  
(Source: Own work)

This procedure is analogous to the Gompertz model (Figure 5):

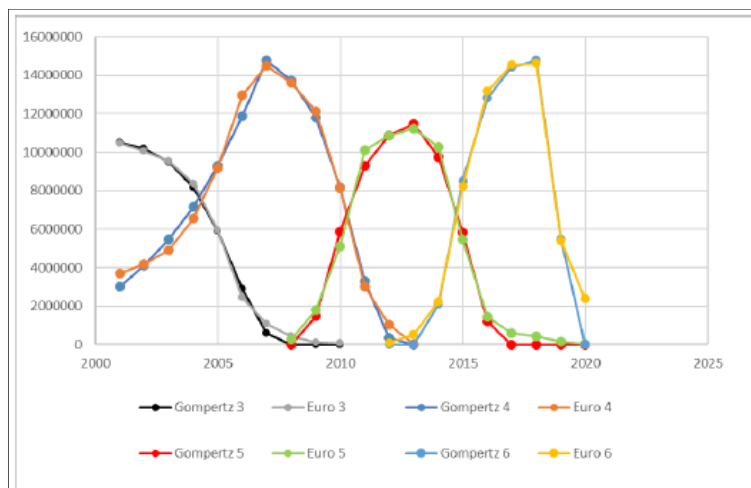


Figure 5. Gompertz Model approximations  
(Source: Own work)

As for the Gaussian Model, since the curve is already bell-shaped, it will only require one approximation (Figure 6):

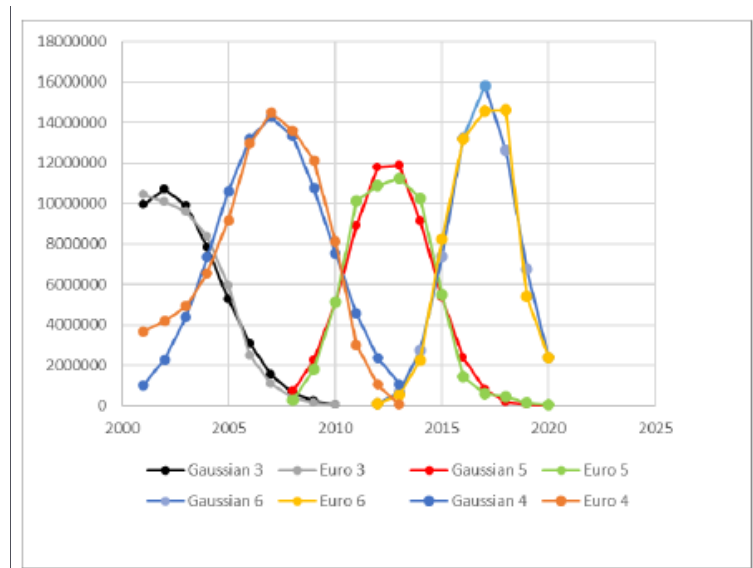


Figure 6. Gaussian Model approximations  
(Source: Own work)

#### 4. Analysis and discussion – prediction

There is no predetermined duration for the Euro Standards. Since the only reference information is the previous standards, the average duration of the past curves will be taken as the future duration for Euro Standard 7. This results in a total of 11 years. The average passenger car sales before the Covid-19 crisis were 14 000 000 vehicles. The future standard is expected to enter into force in 2025. By then, it is reasonable to assume that the vehicle market will have recovered from the past crisis, assuming there will be no future recessions. The prediction will assume that the future curve will be symmetric to simplify the analysis. By plotting the percentage of new vehicles registered for the different past Euro Standards (plotted in *Figure 2*), we obtain each standard's percentage curve of new passenger vehicle registrations.

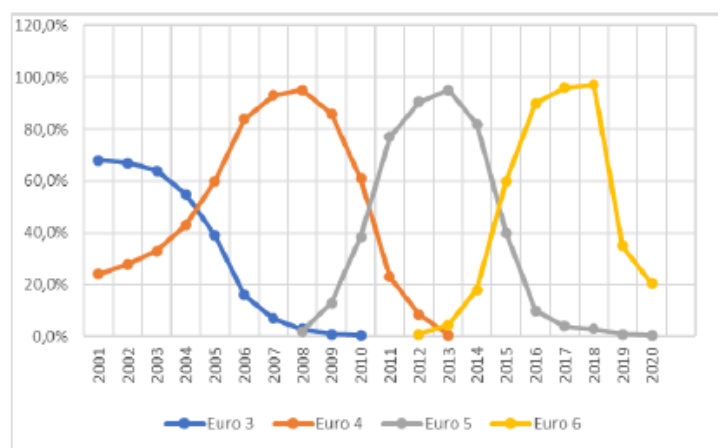


Figure 7. New PC registrations – estimation  
(Source: own estimation based on European vehicle market statistics pocketbook 2021–2022)

##### 4.1 The logistics model prediction

As explained above, the logistic model has three parameters.  $N_0$ , the number of individuals in the population at time  $t = 0$  (130 000);  $K$ , the maximum value attainable by the population (12 000 000) and  $r$ , the growth parameter. The latter depends on the situation at the time. Since it is difficult to determine this parameter, the average of the past curves will



be taken as the future growth coefficient for the Euro 7 curve. Finally, *Figure 8* presents the prediction of the logistic model.

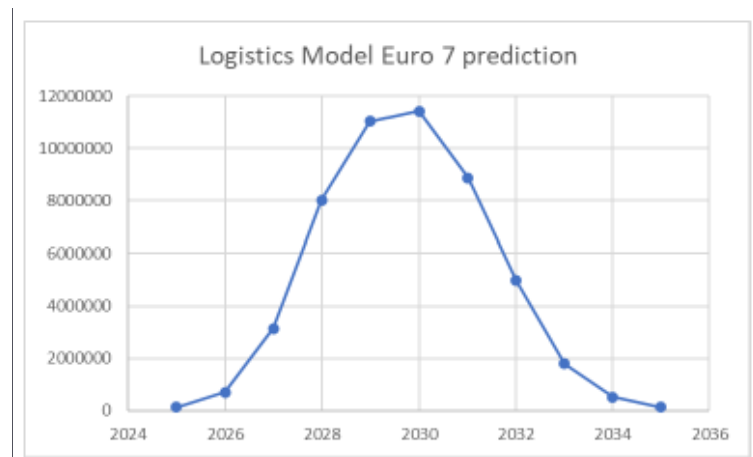


Figure 8. Logistics model prediction  
(Source: own estimation)

#### 4.2 The Gompertz model prediction

This model has three parameters.  $a$  represents the upper limit of the population (12 000 000).  $c$  represents the growth parameter, proceeding in the same way as with the Logistic Model. The remaining parameter is  $b$ , a parameter related to the initial growth. An iterative process has been followed to calculate this parameter. Knowing that the estimated initial value is 130 000, Figure 9 presents the prediction from this model.

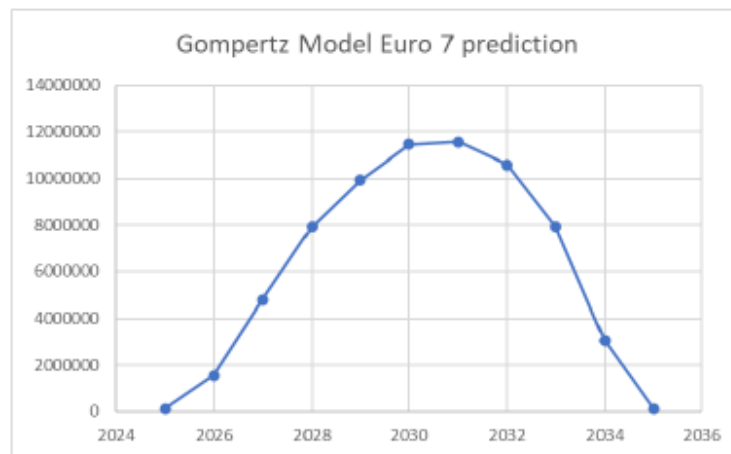


Figure 9. Gompertz model prediction  
(Source: own estimation)

#### 4.3 The Gaussian model prediction

In this model, the parameter  $a$  represents the maximum value of the bell, 12 000 000. The parameter  $b$  affects how the bell falls. The average of the previous curves has been taken, obtaining  $b = 0.12$ . The parameter  $c$  indicates when the maximum value is reached. Symmetry has been assumed in the future curve. According to the prediction, the future curve will last 11 years, with the medium  $c = 6$ .

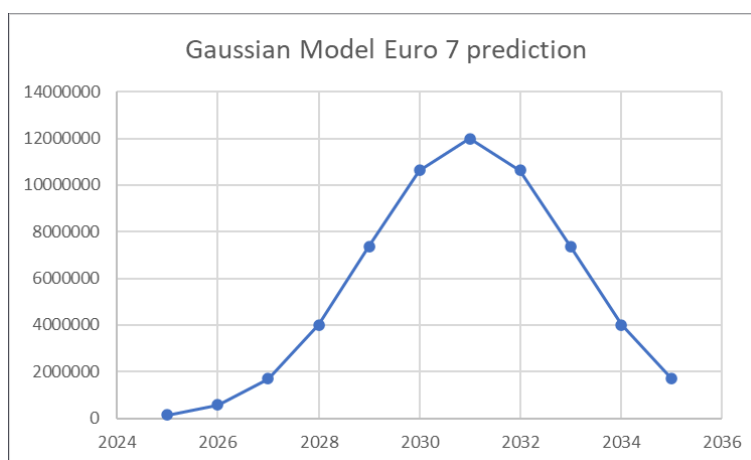


Figure 10. Gompertz model prediction  
(Source: own estimation)

## 5. Conclusion

Table 1 presents the number of new passenger car registrations expected for the new Euro Standard 7 according to the predictions of the three mathematical models.

Table 1. Predictions from Logistics, Gompertz and Gaussian Model for Euro 7

Year	Logistics Model	Gompertz Model	Gaussian Distribution Model
2025	130 000	130 000	150 000
2026	700 000	1 560 000	570 000
2027	3 140 000	4 780 000	1 700 000
2028	8 020 000	7 920 000	4 000 000
2029	11 040 000	9 950 000	7 370 000
2030	11 425 000	11 445 000	10 620 000
2031	8 870 000	11 560 000	12 000 000
2032	4 970 000	10 590 000	10 620 000
2033	1 800 000	7 940 000	7 370 000
2034	510 000	3 060 000	4 000 000
2035	130 000	130 000	1 700 000

Source: Own work

As mentioned above, Euro Standard 7 is expected to come into force in 2025, and the estimated duration is eleven years, until 2035. The analysis has assumed symmetry in the curve, so the registered passenger vehicles should be similar, if not the same, in the start year and the end year. Furthermore, the maximum number of registrations should be reached in 2030. The Gaussian model reaches the maximum number of records in 2031. Moreover, the records in 2035 are much higher than expected. Its prediction has therefore been discarded.



As for the Gompertz model, although its initial and final records coincide with those stipulated, the maximum is reached in 2031, and the progress of registrations is abrupt. Very different from previous curves, so it has also been discarded. Finally, the prediction taken as possible is presented by the Logistic Model. It meets all the above requirements and has a similar growth to the past curves. It should be marked that this analysis has involved several simplifications to facilitate the study. On the other hand, the future is uncertain, unexpected events may occur, and other factors may make this analysis far from reality.

## 6. References

- ACEA – European Automobile Manufacturers’ Association (2022). *Economic and Market Report: State of the EU auto industry – Full-year 2022*. URL: <https://www.acea.auto/publication/economic-and-market-report-state-of-the-eu-auto-industry-full-year-2022/> (7 February 2023)
- Bereczky, Á., Török, Á. (2011). International literature review on the possibilities of biodiesel production. *Periodica Polytechnica Transportation Engineering*. 39(1), 31–37. DOI: <https://doi.org/kjw>
- Für, A., Csete, M. (2010). Modeling methodologies of synergic effects related to climate change and sustainable energy management. *Periodica Polytechnica Social and Management Sciences*. 18(1), 11–19. DOI: <https://doi.org/hbk>
- Lekić, M., Rogić, K., Boldizsár, A., Zöldy, M., Török, Á. (2021). Big Data in logistics. *Periodica Polytechnica Transportation Engineering*. 49(1), 60–65. DOI: <https://doi.org/jc6>
- Radpour, S., Mondal, M. A. H., Paramashivan, D., Kumar, A. (2021). The development of a novel framework based on a review of market penetration models for energy technologies. *Energy Strategy Reviews*. 38, 100704. DOI: <https://doi.org/gq5>
- Rota, F. M., Carcedo, M. J., García, P. J. (2016). Dual approach for modelling demand saturation levels in the automobile market. The Gompertz curve: Macro versus micro data. *Investigación económica*. 75(296), 43–72. DOI: <https://doi.org/jqq6>
- Tánczos, K., Török, Á. (2008). Impact of transportation on environment. *Periodica Polytechnica Transportation Engineering*. 36(1–2), 105–110. DOI: <https://doi.org/fth8bb>
- The International Council On Clean Transport (2021): European Vehicle Market Statistics. Pocketbook 2021/22 URL: <https://theicct.org/wp-content/uploads/2021/12/ICCT-EU-Pocketbook-2021-Web-Dec21.pdf>
- Wang, K. H., Su, C. W., Xiao, Y., Liu, L. (2022). Is the oil price a barometer of China’s automobile market? From a wavelet-based quantile-on-quantile regression perspective. *Energy*. 240, 122501. DOI: <https://doi.org/gpn8z2/>





# Road traffic queue length estimation with artificial intelligence (AI) methods

Csanád Ferencz, Máté Zöldy

 [0000-0002-0177-1646](https://orcid.org/0000-0002-0177-1646),  [0000-0003-1271-840X](https://orcid.org/0000-0003-1271-840X)

*Department of Automotive Technologies, Faculty of Transportation Engineering and Vehicle Engineering,  
Budapest University of Technology and Economics  
Budapest, Hungary  
[csanadferencz@edu.bme.hu](mailto:csanadferencz@edu.bme.hu)*

## Abstract

Sustainable traffic monitoring has always been a significant problem for engineers, queue length being one of the most important metrics required for the performance assessment of signalised intersections. The present study's authors propose a novel approach to estimating cycle-by-cycle queue lengths at a given signalised intersection. Focusing on examining shock wave phenomena and the traffic model, this study first elucidates the definitions and assumptions it employs. Subsequently, it delves into creating the queuing model alongside utilising a machine-learning (ML) based Kalman Filter (KF) algorithm for estimation. The information in the output files is visualised on distinct graphs, along with the velocities at various time intervals derived from virtual simulations involving a queue of 12 vehicles. This graphical representation is a conclusive validation, demonstrating a strong correlation between the simulation and the estimation achieved through the KF approach. The method presented yielded dependable and resilient estimates for the simulated queue lengths, even in the presence of noisy measurements.

## Keywords

autonomous vehicles, artificial intelligence, sustainable mobility, traffic simulation, road network modelling

## 1. Introduction

Traffic signals are the most essential components of urban traffic networks, determining whether passing traffic at a junction should go or stop (Lee et al., 2015). These signal transition operations may lead to periodic changes in the queuing process, thus affecting urban traffic flow reliability (Schrank et al., 2015). Hence, when considering signal control optimisation and evaluating performance at signalised intersections, the significance of an accurate and resilient queue length estimation method cannot be overstated (Goodall et al., 2013). Because supplementary performance metrics like stops, travel time, and vehicle delay can be inferred by leveraging queue length data, these performance indicators will serve as valuable tools for traffic management, thus improving the level of service for the entire urban traffic network (Wang et al., 2019).

Road traffic queue length estimation is a crucial measurement of traffic signal control at any given urban intersection (Cao and Zöldy, 2020). However, conventional queue length estimation methods mainly rely on fixed detectors and use point detector data (Viti et al., 2010). These methods often struggle to handle scenarios with long queues that extend beyond the location of the point sensor (Sharma et al., 2007). Additionally, their focus tends to be on average queue lengths rather than considering the spatial and temporal distributions of queues (Fuliang et al., 2017). However, recent efforts have been substantial in developing precise and dependable techniques for queue length estimation at signalised intersections (Wu and Liu, 2011). The current study introduces a novel approach for estimating cycle-by-cycle queue lengths at a specific signalised intersection. This approach is particularly suited for addressing traffic challenges on a regional scale, thereby contributing to the sustainable development of intelligent transportation systems.

Following a concise examination of existing literature concerning queue length estimation at signalised intersections, with a specific emphasis on scrutinising shock wave phenomena and traffic models, this study outlines the definitions and assumptions employed. Subsequently, the creation of the queuing model is detailed, and the methodology for queue length estimation is introduced. This involves a machine-learning (ML) approach, specifically employing the Kalman Filter (KF)



algorithm. Finally, the proposed method's result validation is also presented based on parameter estimation and traffic simulation.

## 2. Literature review

Real-time traffic control is vital in managing transportation, spanning urban and rural areas (Zöldy and Baranyi, 2021). Consequently, continuous measurement of every traffic parameter has become pivotal. Typically, estimation models are employed to skillfully reconstruct and foresee current and future traffic conditions based on collected information (Ferencz and Zöldy, 2021). However, the logistical and financial impracticality of placing sensors extensively across roadways renders it unfeasible (Wu and Yang, 2013). The number of measurement devices at road sections is limited to employ the minimal number of fixed sensors to curtail costs while maximising data collection (Yao and Tang, 2019). Nevertheless, this reduced sensor count yields fewer data points, amplifying uncertainty within the estimation model (Horváth and Tettamanti, 2021). Addressing this uncertainty effectively entails the application of robust methodologies, exemplified by the approach employed in this current study.

Traffic queue length estimation approaches for signalised intersections are commonly classified into two main categories: methods rooted in the input-output cumulative plot analysis and methods grounded in the principles of the shock wave theory (Liu et al., 2019). The former approach primarily infers queue lengths by examining the patterns of vehicle arrivals and departures at intersections. However, this study will investigate the latter type of estimation method in depth (Cetin, 2012).

In order to analyse shock wave phenomena, the so-called road traffic fundamental diagram theory can be used. Shock waves form in traffic (Tettamanti, 2021), when there is a sudden reduction or increase in the capacity of a roadway (Figure 1), for instance, when traffic stops at a red light (Varga and Tettamanti, 2023), in the case of an accident, or even lane reduction on a multi-lane road (Figure 2).

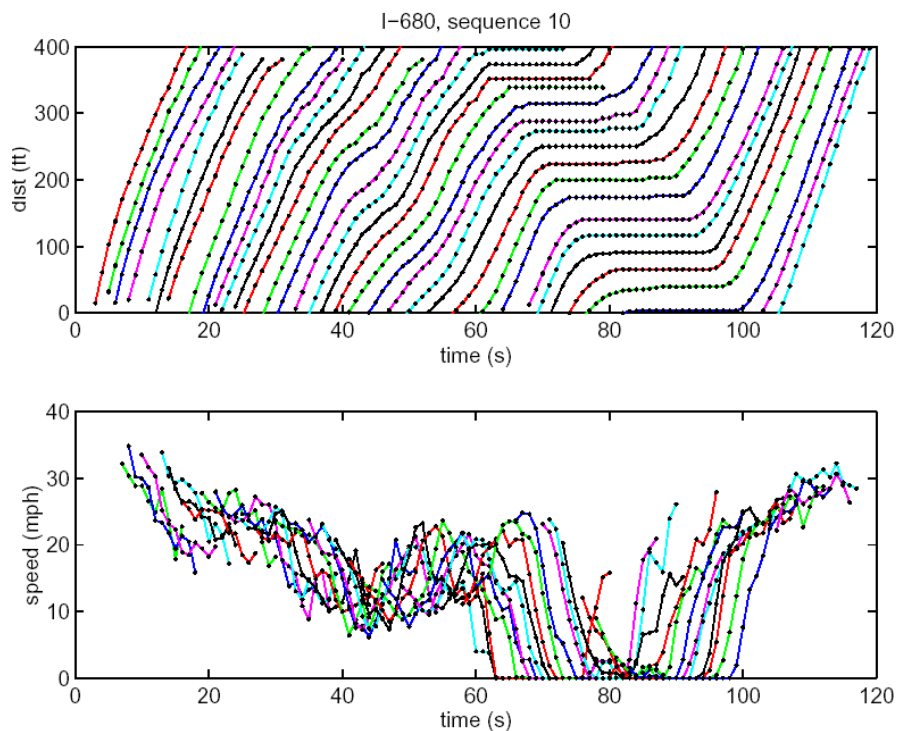


Figure 1 Shockwave profile model on freeway (Tettamanti, 2021)



Applying the methods based on the shock wave theory, one can profile the stopping and discharging shockwaves based on detector data, consequently providing spatial and temporal information on the queues (Ibrahim et al., 2019). This data will encompass both the maximum and residual queue lengths (Cai et al., 2014).

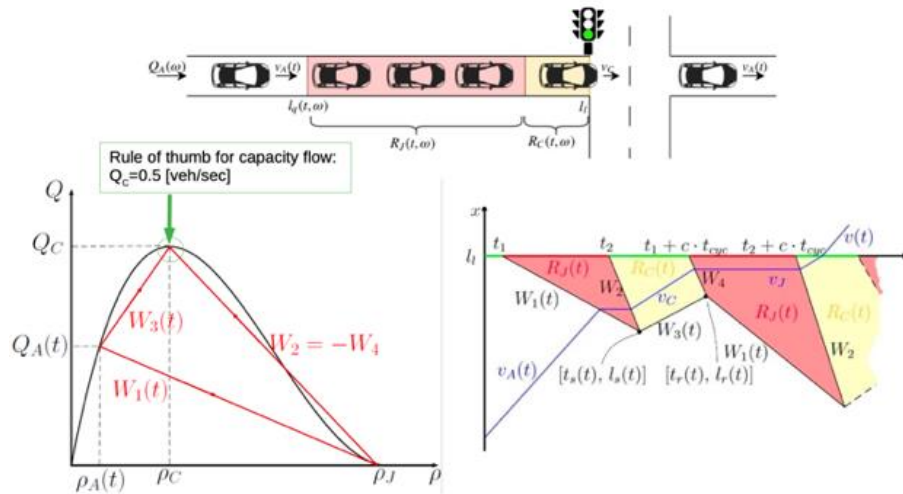


Figure 2. Special case fundamental diagram for queuing at traffic light (Tettamanti, 2021)

### 3. Problem definition

The main target of this study is to create a shockwave profile model as a queueing model at a signalised intersection. In order to do this, the main task is divided into four subtasks, each one presented in the corresponding section of the paper, as follows:

- Creation of a queueing model at a signalised intersection,
- Creation of SUMO network with traffic lights,
- Creation of logs of vehicle trajectories or queue lengths and parameter estimation with machine learning-based technique of the queueing model,
- Result validation with SUMO.

For these tasks in terms of software, the SUMO v1.8.0 microscopic road traffic simulator was used for network creation and simulation, respectively. MATLAB\_R2019b was applied for the creation of the queueing model and for the machine learning parameter estimation.

### 4. Queueing model creation at a signalised intersection

Traffic simulations supported the present study in the SUMO (Simulation of Urban Mobility) road traffic simulation software. At the same time, the short-term TraCI protocol for “Traffic Control Interface” gives access to a running road traffic simulation, allowing the retrieving of simulated objects' values and manipulating their behaviour “online”.

In a general context, a stop-and-go wave, commonly referred to as a shockwave profile model, can be described as a phenomenon where vehicles slow down or halt sequentially. It is possible to leverage vehicle trajectory data to gauge these shockwaves' propagation speed within a microscopic framework. In the case of this present study, however, a particular queueing model was implemented, similar to the shockwave model (Tettamanti et al., 2019).

Commencing from a stationary stance, a vehicle will undergo maximum acceleration if there are no vehicles ahead. As its velocity increases, the acceleration will diminish until it reaches zero. Conversely, when a vehicle approaches an obstacle like a red light or another vehicle, it will decelerate until its speed reaches 0 [m/time-step], which defines how many vehicles are waiting in a queue approaching a red traffic light (Akçelik, 2001). After the initialisation and setting of the visualisation scheme, we define the main loop of the MATLAB queueing model (see *Algorithm 1*), a sequence going from the start 0, utilising ten simulation steps per second (car following model), to 240 time-steps.



**Algorithm 1**

```

while i <= 120*10 + 1
    traci.simulationStep();
    vehicles= traci.vehicle.getIDList();
    for ii=1:length(vehicles)
        traci.vehicle.setSpeedMode(cell2mat(vehicles(ii)),0);
        leader=traci.vehicle.getLeader(cell2mat(vehicles(ii)));
        D(ii,i)=traci.vehicle.getDistance(cell2mat(vehicles(ii)));
        Sp(ii,i)=traci.vehicle.getSpeed(cell2mat(vehicles(ii)));
        if (~isempty(leader))
            l = traci.vehicle.getPosition(leader);
            dist=traci.vehicle.getDrivingDistance2D(cell2mat(vehicles(ii)),l(1), l(2));
            if (dist <= 10) %stop
                speed = traci.vehicle.getSpeed(leader);
            elseif ((dist>=50) && (traci.vehicle.getSpeed(cell2mat(vehicles(ii)))== 0))
                speed = 10; else
                speed = 10; end
            else
                speed = 10; end
            nextTLS = traci.vehicle.getNextTLS(cell2mat(vehicles(ii)));
            if (~isempty(nextTLS))
                distanceToNextTLS = nextTLS{1,1}{1,3};
                stateOfNextTLS = nextTLS{1,1}{1,4};
                if ((distanceToNextTLS <=4) && (stateOfNextTLS == 'r'))
                    traci.vehicle.setSpeed(cell2mat(vehicles(ii)),0);
                elseif ((distanceToNextTLS <=10) && (distanceToNextTLS >4))
                    traci.vehicle.setSpeed(cell2mat(vehicles(ii)),speed/2);
                elseif ((distanceToNextTLS <=4) && (stateOfNextTLS == 'g'))
                    traci.vehicle.setSpeed(cell2mat(vehicles(ii)),speed); else
                    traci.vehicle.setSpeed(cell2mat(vehicles(ii)),speed); end
            end
            i=i+1;
        end
    end
end

```

After that comes the definition of the queuing model at a signalised intersection in a MATLAB file, basically the model’s main control algorithm. This is associated and interconnected with the TraCI program file containing the error handling (in which the remote port is also defined) and creating an output file containing queue parameters, step length.

Here in this sequence, firstly we define the TraCI simulation step, create a vehicle ID list, and then within a sequence going all the way from 1 to the arbitrary length of the vehicles (total number of 12 cars), we set the vehicle speeds (0 [m/time-step] for queuing, 5 [m/time-step] for approaching status and 10 [m/time-step] for moving status), starting with and based on the leading vehicle, as well as based on the traffic light signals and distances to these (<=4 [m], >4 [m], or <=10 [m]), thus obtaining a more-or-less similar, customised shockwave profile queuing model.

The TraCI program file encompasses 15 distinct SUMO object folders (such as vehicles and routes), each containing ‘get’ and ‘set’ functions linked to the respective object. The typical framework for ‘get’ or ‘set’ operations also involves the domain (object name) and the methods for retrieving (‘get’) or altering (‘set’) the attributes of the targeted object. Upon launching the main control script file, the basic TraCI program becomes accessible. Another important thing is to check whether we have the same port number in the TraCI program and control script files. Otherwise, the MATLAB code will fail (SUMO User Documentation, 2021).

**5. Simple SUMO network with traffic lights**

From the SUMO network’s perspective, we can gain additional information about the observed system if proper modelling is also involved (see Figure 3 below). When it comes to connecting the nodes with edges (see *Algorithm 2*), it has to be mentioned that edges are directed. Each vehicle enters an edge at the node given as *from* and ends at the node given as *to*.

**Algorithm 2**

```

<additional>
    <route id="route2" edges="4to1 1to2 2to3 3to4 4to5 5to6 6to7 7to4 4to1"/>
    <rerouter id="rerouter_0" edges="4to1">
        <interval end="1e9">
            <routeProbReroute id="route2"/>
        </rerouter>
    </additional>

```

After that, we will specify the number of vehicles, their ID, distinguishing colours, start or departure positions, the driving route, acceleration, deceleration, and speed of these cars, respectively. We will set a delay value of 100 [ms] as well.

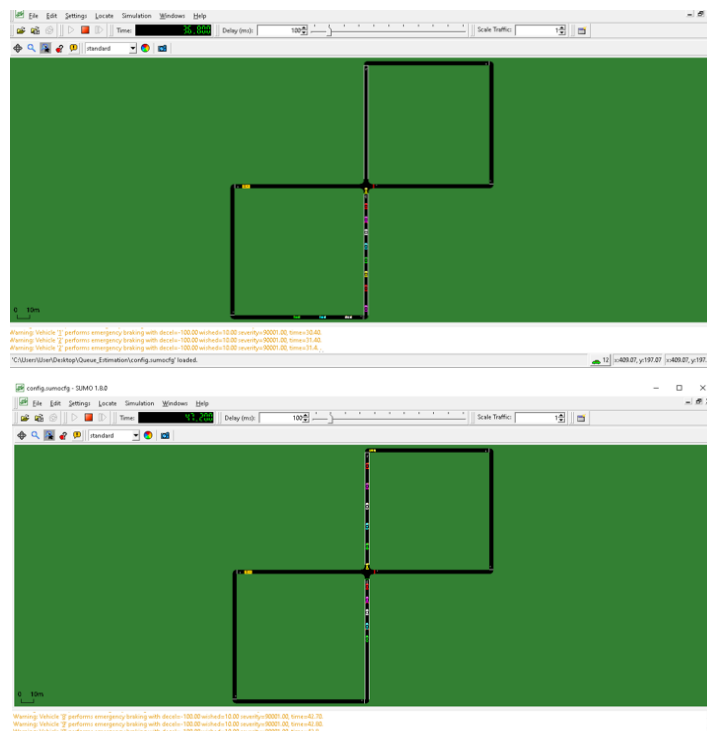


Figure 3 SUMO network with traffic lights at two different time-steps (Own work, 2023)

Once we have all the nodes and edges of the traffic network, we can generate our SUMO road traffic network (Road Traffic Control Laboratory BME, 2021). In *Algorithm 3*, we define all the routes of this network.

**Algorithm 3**

```

<routes>
  <vType id="type1" accel="10" decel="10" sigma="0.5" length="5" maxSpeed="20"/>
  <route id="routel" edges="1to2 2to3 3to4 4to5 5to6 6to7 7to4 4to1"/>
  <vehicle id="0" type="type1" route="routel" depart="0" color="1,1,0"/>
  <vehicle id="1" type="type1" route="routel" depart="2.0" color="1,0,0"/>
  <vehicle id="2" type="type1" route="routel" depart="4.0" color="1,0,1"/>
  <vehicle id="3" type="type1" route="routel" depart="6.0" color="1,1,1"/>
  <vehicle id="4" type="type1" route="routel" depart="8.0" color="0,1,1"/>
  <vehicle id="5" type="type1" route="routel" depart="10.0" color="0,1,0"/>
  <vehicle id="6" type="type1" route="routel" depart="12.0" color="1,1,0"/>
  <vehicle id="7" type="type1" route="routel" depart="14.0" color="1,0,0"/>
  <vehicle id="8" type="type1" route="routel" depart="16.0" color="1,0,1"/>
  <vehicle id="9" type="type1" route="routel" depart="18.0" color="1,1,1"/>
  <vehicle id="10" type="type1" route="routel" depart="20.0" color="0,1,1"/>
  <vehicle id="11" type="type1" route="routel" depart="22.0" color="0,1,0"/>
</routes>

```

In *Algorithm 4* below, the SUMO network for the simulation and configuration of the intersection are defined and built: the nodes (junctions), edges (streets connecting the junctions), connections and routes, input and output files, as well as the number of vehicles, position and settings of the traffic lights (every 12-simulation step changing red and green light, yellow is omitted for simplicity reasons). In the *Algorithm 4* configuration file, the *Algorithm 2* and *Algorithm 3* scripts are glued together, obtaining a final configuration file for the SUMO simulation (Road Traffic Control Laboratory BME, 2021).



#### Algorithm 4

```

<configuration>
  <input>
    <net-file value="network.net.xml"/>
    <route-files value="routes.rou.xml"/>
  </input>
  <processing>
    <time-to-teleport value="-1"/>
  </processing>
  <report>
    <xml-validation value="never"/>
    <duration-log.disable value="true"/>
    <no-step-log value="true"/>
  </report>
  <time>
    <begin value="0"/>
    <end value="10"/>
  </time>
  <gui-settings-filevalue="gui settings.cfg"/>
  <additional-files value="add.xml"/>
</configuration>

```

Finally, we will output all the necessary parameters of the queueing model to validate the obtained results with the machine learning-based parameter estimation described in the following section. These parameters are the vehicle IDs and their position and speed for different time steps. If a given vehicle's speed is 0 [m/time-step], we will consider it waiting in a queue at a traffic light. Thus, it can be determined for how long and how many vehicles are at a given signalised intersection queueing.

### 6. Queue length estimation with ML technique

The present section introduces practical estimation tools for road traffic measurements, specifically for a signalised intersection queueing scenario. The presented method is a Kalman Filter (KF)-based queue length estimation technique, contributing to a better measurement by filtering the raw data.

The KF algorithm consists of two main stages: prediction and correction. Accordingly, there are two groups of equations in the algorithm: the prediction equations, which produce a state estimate and the extrapolation of estimate error covariance for the next step – the a priori estimation – and the correction equations, which recalculate the state estimate and estimate error covariance based on the updated measurement values – a posteriori estimation (Yin et al., 2018).

To employ the Kalman Filter for estimating the inner state of processes based solely on a sequence of noisy observations (Terra et al., 2014), it is necessary to formulate the process by defining the matrices for each time step  $k$  (Ishihara et al., 2006). The KF model postulates that the true state at time  $k$  develops from the state at  $k - 1$  as outlined in (1):

$$x_k = F_k x_{k-1} + B_k u_k + w_k \quad (1)$$

where,

$F_k$  – state transition model applied to the preceding state  $x_{k-1}$ ,

$B_k$  – control-input model employed on the control vector  $u_k$ ,

$w_k$  – process noise, hypothesised to originate from a zero-mean multivariate normal distribution  $\mathcal{N}$  with covariance  $Q_k$ , as presented in (2):

$$w_k \sim \mathcal{N}(0, Q_k) \quad (2)$$



At time step  $k$ , an observation (measurement)  $z_k$  of the true state is acquired, as described by (3):

$$z_k = H_k x_k + v_k \tag{3}$$

where,

$H_k$  – observation model that maps the true state space into the observed space,

$v_k$  – observation noise assumed to be zero-mean Gaussian white noise, with the observation noise covariance  $R_k: v_k \sim \mathcal{N}(0, R_k)$ .

The initial state, as well as the noise vectors at each step  $\{x_0, w_1, \dots, w_k, v_1, \dots, v_k\}$  are all considered to be mutually independent. The filter’s state is described by (4), (5), (6) and (7), while the *Optimal* Kalman gain is defined by (8).

$$x_{k|k} = \hat{x}_{k|k-1} + K_k \tilde{y}_k \tag{4}$$

$$P_{k|k} = (I - K_k H_k) \hat{P}_{k|k-1} \tag{5}$$

$$\hat{x}_{k|k-1} = F_k x_{k-1|k-1} + B_k u_k \tag{6}$$

$$\hat{P}_{k|k-1} = F_k P_{k-1|k-1} F_k^T + Q_k \tag{7}$$

$$K_k = \hat{P}_{k|k-1} H_k^T S_k^{-1} \tag{8}$$

where,

$x_{k|k}$  – *a posteriori* state estimate at time  $k$ , given observations up to and including at time  $k$ ,

$P_{k|k}$  – *a posteriori* estimate covariance matrix, representing the measure of estimated accuracy of the state estimate,

$\hat{x}_{k|k-1}$  – predicted (*a priori*) state estimate,

$\hat{P}_{k|k-1}$  – predicted (*a priori*) estimate covariance,

$B_k$  – control–input model,

$F_k$  – state–transition model,

$H_k$  – observation model,

$Q_k$  – covariance of process noise.

The following steps will be defined for the operation of the KF algorithm at each time-step for the prediction phase:

1. Calculating the a priori state estimation by using measured values,
2. Calculating the a priori error covariance.

Similarly, for the correction phase, we can define the following steps:

1. Calculating  $y_k$  based on measurement,
2. Calculating the a posteriori state estimation,
3. Calculating the a posteriori error covariance,
4. Increment step index and go to step 1 of the prediction phase.

As vehicles navigate through the intersection, two distinct motion statuses have been defined in the current context: queuing and moving. The queuing status pertains to vehicles that approach with a speed near 0 or come to a complete stop behind the queue. On the other hand, the moving status relates to vehicles that are in motion at a specified speed.



The rear of the queue is determined as the location of the last vehicle among all those in queuing status at a specific time step. Queue length signifies the overall count of vehicles in the queuing status for a lane at a specific time step. The maximum queue length is the maximum value among the lengths observed within a given cycle.

The Kalman Filter estimation is implemented in a separate script file. The code starts with initialising and loading the output files created at the end of the main control script containing the different distance and speed values. The Kalman Filter utilises driving distances to forecast the velocity of vehicles.

The output of the distances file contains a  $12 \times 1201$  measurement matrix, with the help of which we can estimate the vehicle speeds. The simulation is running with 12 vehicles. The speed data file is mainly used to calculate the queue lengths from the simulation. The simulated queue lengths must be calculated to validate the estimated data. This file contains a  $12 \times 1201$  validation matrix used to calculate the simulated queue lengths for validation.

According to the model, the queuing vehicle speed is considered 0 [m/time-step], but considering the Kalman Filter's tolerance error, we calculate with a queuing velocity of less than 2 [m/time-step].

After the initialisation phase, the Kalman Filter calculates the velocity of the vehicle based on the driven distance for each time-step. *Algorithm 5* below displays the Kalman Iteration steps, where:

- $Z$  represents the measurement vector, where  $Z = \text{Simulated Data} + \text{Random Gaussian Noise}$ ,
- $\Phi$  characterises the dynamics of the vehicle, serving as the motion equation,
- $K$  stands for the Kalman gain, where if  $K$  is low, more weight goes to the model prediction. If  $K$  is large, more weight goes to the measurement,
- $Q$  signifies the process noise covariance, indicating the level of uncertainty inherent in the model,
- $M$  stands for the measurement matrix,
- $R$  denotes the measurement noise covariance,
- $Xk\_buffer$  is used for later display, it is a  $2 \times 1201$  matrix in which the first row contains the estimated driven distance values, and the second row contains the estimated speed values for each time-step.

Algorithm 5

```
% Kalman iteration
for k=1:Nsamples
    % Z is the measurement vector
    Z = Xtrue(k+1)+sigma_meas*randn;
    Z_buffer(k+1) = Z;
    % Kalman iteration
    P1 = Phi*P*Phi' + Q;
    S = M*P1*M' + R;
    % K is Kalman gain.
    K = P1*M'*inv(S);
    P = P1 - K*M*P1;
    Xk=Phi*Xk_prev + K*(Z-M*Phi*Xk_prev);
    Xk_buffer(:,k+1) = Xk;
    % For the next iteration
    Xk_prev = Xk;
end
```

This estimation is calculated for every vehicle in the model by embedding the Kalman Filter estimation in a for loop, which iterates over all vehicles. The estimated value provided by the KF is always an expected value with a standard deviation. After the iteration, the queue lengths are calculated. The calculation begins after the last vehicle enters the network. The queue lengths are calculated from the simulated and estimated speed dataset by iterating over the velocities and calculating the number of queuing vehicles at each time-step (see *Algorithm 6*):





**Algorithm 6**

```

% Queue lengths for each iteration, if speed is lower than 2, the vehicle is assumed to be in a queue
for col = 250:1201
    queueLengthEst = 0;
    queueLengthSim = 0;
    for row = 1:12
        if (Xk_sum(row,col) < 2)
            queueLengthEst=queueLengthEst+1;
        end
        if (Sp(row,col) < 2)
            queueLengthSim=queueLengthSim+1;
        end
    end
    queueLengths(1,col) = queueLengthEst;
    queueLengths(2,col) = queueLengthSim;
end

```

**7. Result validation**

The results were validated with the Kalman Filter-based parameter estimation technique of the queuing model in MATLAB.

In Figure 4, the estimated driving distances for the 12 vehicles are displayed in red, along with the measured distance of driving of the last vehicle plotted in blue. The figure also shows the estimated queue lengths for each time-step displayed in red and the simulated queue lengths in blue.

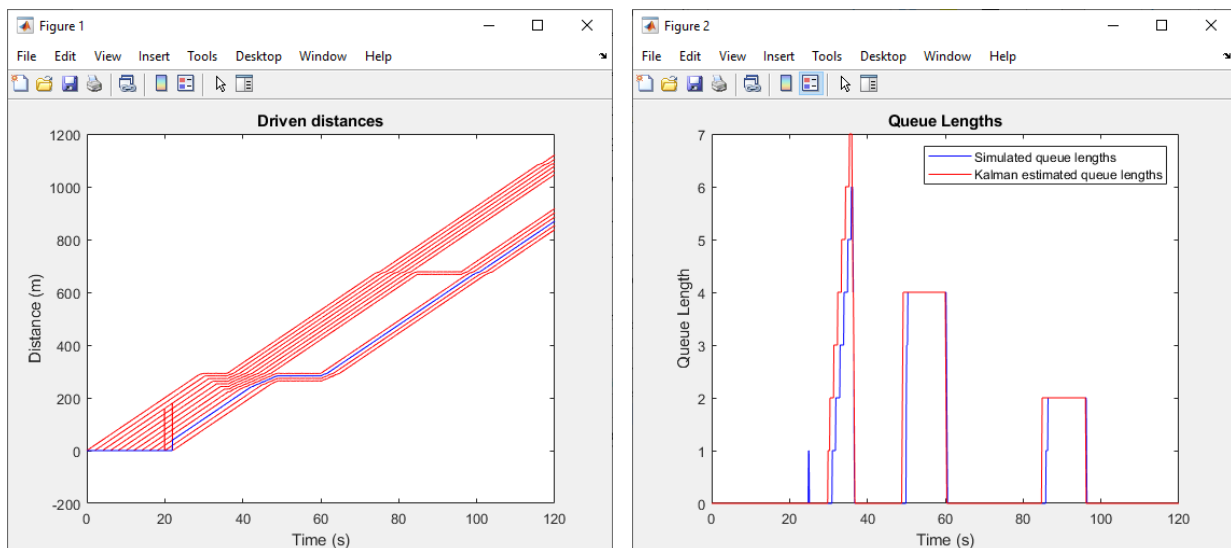


Figure 4 Estimated driving distances and simulated queue lengths (Own work, 2023)

The data in the output files are plotted on two different graphs, together with the speeds at different time-steps obtained from the SUMO simulation for all 12 vehicles, consequently achieving a clear diagram-based result validation showing a close relation between simulation and estimation.

**8. Conclusions**

The sustainable progress of urban mobility faces obstacles from traffic congestion, traffic accidents, and environmental pollution. Recent research in road traffic engineering, particularly concerning signalised intersections where congestion often accumulates, indicates a growing focus on real-time estimation of motor vehicle queue lengths using the shock wave theory. These approaches are frequently employed with high-resolution loop detector data or probe vehicle information. Here, a novel approach was presented, through which cycle-by-cycle queue lengths were estimated at a given signalised intersection.

Based on analysing and creating the shock wave profile model, the definitions and assumptions used in this study were described, followed by the queuing model and network creation with traffic lights, creation of logs of vehicle trajectories or queue lengths, parameter estimation with a machine-learning based Kalman Filter algorithm, as well as virtual simulation and numerical method based result validation. Despite the noisy measurements, the presented method gave robust and reliable estimation results of the simulated queue lengths.

Future research has to focus on more detailed modelling of the network traffic by considering a more comprehensive simulation of queue length evolution and more precise dynamics of the residual queue. Furthermore, it is important to



consider sensible enhancements for accurately estimating the residual queue length. In this context, various shockwaves can depict the vehicle arrivals, including whether they assimilate into the queue's rear when the last vehicle is stationary or in motion. Additionally, a more comprehensive calculation of the departure shockwave can be achieved by incorporating assumptions about its stochastic characteristics.

Limitations of the proposed model and algorithms also have to be considered. Future research may enhance the suggested models' precision by utilising more extensive simulated datasets and advanced statistical methodologies (Henrickson et al., 2015).

### Acknowledgement

The realisation of this present scientific research project would not have been possible without the support of the Department of Automotive Technologies of the Budapest University of Technology and Economics.

### References

- Akçelik, R. (2001). *HCM 2000 Back of Queue Model for Signalized Intersections*. Akçelik & Associates Pty. Ltd., Melbourne, Australia.
- Cai, Q., Wang, Z., Zheng, L., Wu, B. Wang, Y. (2014). Shock wave approach for estimating queue length at signalised intersections by fusing data from point and mobile sensors. *Transportation Research Record: Journal of the Transportation Research Board*.2422(2), 79–87. DOI: <https://doi.org/bkphhn>
- Cao, H., Zöldy, M. (2020). An investigation of autonomous vehicle roundabout situation. *Periodica Polytechnica Transportation Engineering*. 48(3), 236–241. DOI: <https://doi.org/hg4m>
- Cetin, M. (2012). Estimating queue dynamics at signalised intersections from probe vehicle data: Methodology based on kinematic wave model. *Transportation Research Record*. 2315(1), 164–172. DOI: <https://doi.org/gjh7th>
- Ferencz, Cs., Zöldy, M. (2021). driving cycle modeling, simulation and validation on 1: 10 scale vehicle model platform [In Hungarian: Autónm menetciklus-modellezés,-szimuláció és-validálás 1: 10-es méretarányú járműmodell-platfomon: Autonomous]. *29th International Conference on Mechanical Engineering*. 29, 208–212.
- Fuliang, L., Keshuang, T., Jiarong, Y. Keping L. (2017). Real-Time Queue Length Estimation for Signalized Intersections Using Vehicle Trajectory Data. *Transportation Research Record: Journal of the Transportation Research Board*. 2623, 49–59. DOI: <https://doi.org/gdjers>
- Goodall, N. J., Smith, B. L. and Park, B. (2013). Traffic Signal Control with Connected Vehicles. *Transportation Research Record: Journal of the Transportation Research Board*. 2381, 65–72. DOI: <https://doi.org/gcvj4f>
- Henrickson, K., Zou, Y., Wang, Y. (2015). Flexible and robust method for missing loop detector data imputation. *Transportation Research Record: Journal of the Transportation Research Board*. 2527, 29–36. DOI: <https://doi.org/gqcggh>
- Horváth, M., Tettamanti T. (2021). Robust vehicle count estimation on urban signalised links. *Measurement*. 181, 109581. DOI: <https://doi.org/kvf8>
- Ibrahim, A., Cicic, M., Goswami, D., Basten, T., Johansson, K. (2019). Control of Platooned Vehicles in Presence of Traffic Shock Waves, *2019 IEEE Intelligent Transportation Systems Conference (ITSC)*. 1727–1734. DOI: <https://doi.org/gh95kw>
- Ishihara, J. Y., Terra, M. H., Campos, J. C. T. (2006). Robust Kalman Filter for Descriptor Systems. *IEEE Transactions on Automatic Control*. 51(8), 1354. DOI: <https://doi.org/bm5w3g>
- Lee, S., Wong, S. C., Li, Y. C. (2015). Real-Time Estimation of Lane-Based Queue Lengths at Isolated Signalized Junctions. *Transportation Research Part C: Emerging Technologies*. 56, 1–17. DOI: <https://doi.org/t7hr8w>
- Liu, H., Wu, X., Ma, W., Hu, H. (2019). Real-time queue length estimation for congested signalised intersections. *Transportation Research Part C: Emerging Technologies*. 17(4), 412–427. DOI: <https://doi.org/dprtn9>
- Road Traffic Control Laboratory BME (2021). *Simple example code with MATLAB*. URL: <http://kjit.bme.hu/index.php/en/kutatas-traffic-en/sumotraci-en>
- Road Traffic Control Laboratory BME (2021). *The beginning steps of SUMO TRACI COM programming with MATLAB*. URL: [http://kjit.bme.hu/images/traffclab/Research/SUMOTRACI/MATLAB\\_TraCI.pdf](http://kjit.bme.hu/images/traffclab/Research/SUMOTRACI/MATLAB_TraCI.pdf)
- Schrank, D., Eisele, B., Lomax, T (2015). 2014 Urban Mobility Scorecard. *Texas A&M Transportation Institute*, College Station, 2015.3.
- Sharma, A., Bullock, D. M., Bonneson, J. A. (2007). Input-Output and Hybrid Techniques for Real-Time Prediction of Delay and Maximum Queue Length at Signalized Intersections. *Transportation Research Record: Journal of the Transportation Research Board*. 2035, 69–80. DOI: <https://doi.org/fw429g>
- SUMO User Documentation (2021). *TraCI overview*. URL: [https://sumo.dlr.de/docs/TraCI.html#traci\\_commands](https://sumo.dlr.de/docs/TraCI.html#traci_commands)
- Terra, M. H., Cerri, J. P., Ishihara, J. Y. (2014). Optimal Robust Linear Quadratic Regulator for Systems Subject to Uncertainties. *IEEE Transactions on Automatic Control*. 59(9), 2586–2591. DOI: <https://doi.org/kvf9>
- Tettamanti, T. (2021). Fundamental Diagram of Traffic Flow. Master Program Course Autonomous Vehicle Control Engineer. Budapest University of Technology and Economics, Faculty of Transportation Engineering and Vehicle Engineering, Budapest. INTFIN Course Material supported by EMMI 32708-2/2017. (Downloaded: 2 May 2023 12:43)
- Tettamanti, T., Luspai, T., Varga, I. (2019). *Road Traffic Modeling and Simulation*. Akadémiai Kiadó, Budapest.
- Varga, B., Tettamanti, T. (2023). Jam Propagation Analysis With Mesoscopic Traffic Simulation. *IEEE Transactions on Intelligent Transportation Systems*. pp. 1-12. DOI: <https://doi.org/kwgg>
- Viti, F., Van Zuylen, H. J. (2010). Probabilistic Models for Queues at Fixed Control Signals. *Transportation Research Part B: Methodological*. 44(1), 120–135. DOI: <https://doi.org/dv7t7s>
- Wang, S., Huang, W., Lo, H. (2019). Traffic parameters estimation for signalised intersections based on combined shockwave analysis and Bayesian network. *Transportation Research Part C: Emerging Technologies*. 104, 22–37. DOI: <https://doi.org/gf5t9g>
- Wu, A., Yang, X. (2013). Real-time queue length estimation of signalised intersections based on RFID data. *Procedia – Social and Behavioral Sciences*. 96, 1477–1484. DOI: <https://doi.org/kvgb>
- Wu, X., Liu, H. (2011). A Shock Wave Profile Model for Traffic Flow on Congested Urban Arterials. *Transportation Research Part B: Methodological*, 45, No. 10, 1768–1786. DOI: <https://doi.org/dpjxq>



- Yao, J., Tang, K. (2019). Cycle-based queue length estimation considering spillover conditions based on low-resolution point detector data. *Transportation Research Part C: Emerging Technologies*. 109, 1–18. DOI: <https://doi.org/kv9c>
- Yin, J., Sun, J., Tang, K. (2018). A Kalman Filter-Based Queue Length Estimation Method with Low-Penetration Mobile Sensor Data at Signalized Intersections. *Transportation Research Record: Journal of the Transportation Research Board*. DOI: <https://doi.org/gffh6j>
- Zöldy, M., Baranyi, P. (2021). Cognitive Mobility – CogMob. *12th IEEE International Conference on Cognitive Infocommunications – CogInfoCom 2021*. Proceedings IEEE, 921–925. URL: [https://www.researchgate.net/publication/361435417\\_Cognitive\\_Mobility\\_-\\_CogMob](https://www.researchgate.net/publication/361435417_Cognitive_Mobility_-_CogMob)



# Technical and economic viability of hydrogen road vehicles in Valencia, Spain

David Pla Benralte  
Universitat Politècnica de València  
Valencia, Spain  
[dplaber@etsii.upv.es](mailto:dplaber@etsii.upv.es)

## Abstract

Decarbonising the automotive industry is important in improving air quality by reducing emissions. As one of the main promising alternatives to achieve this, hydrogen technologies are emerging. This paper will analyse the hydrogen automotive market, studying the economic and functional feasibility of implementing a plan to introduce hydrogen vehicles in society. The necessary supply is estimated, as well as the green production of the required hydrogen through the investigation of a plant to produce this gas using solar energy. This way, a vision of the future of hydrogen technologies applied to automation and its possible introduction to society will be obtained.

## Keywords

hydrogen vehicles, electrolysis, fuel cell, FCEV, solar energy.

## 1. Introduction

The decrease in the impact of automotive pollution on our planet by reducing vehicle emissions (*Zalacko et al., 2021*) is unquestionable. Decarbonisation will be key to achieving this (*Torok et al., 2014*). In this sense, one of the most promising and increasingly viable solutions is the implementation of hydrogen cars (*Zöldy, 2009*). These vehicles use fuel cells that convert hydrogen into electricity, emitting no polluting gases. Moreover, hydrogen is a renewable and abundant resource on our planet, which makes it a sustainable option in the long term (*Szendrő, Csete, Török, 2012*). However, despite the advantages of hydrogen cars, their implementation presents significant challenges, such as the need for infrastructure for hydrogen production, storage, and distribution or willingness to use (*Andrejszki et al., 2015*) or safety-related questions (*Ágoston and Madleňák, 2021*). Therefore, this paper will analyse the hydrogen automotive market, studying the economic and functional feasibility of implementing a plan to introduce hydrogen vehicles. The necessary supply and the green production of the required hydrogen will be explored by investigating a plant to produce this gas using solar energy in Valencia, Spain. This way, a vision of the future of hydrogen technologies applied to automation and its possible introduction to society will be obtained.

## 2. Data and methods

### 2.1. Plans description

This paper focuses on the Spanish city of Valencia, where the data show that there will be 1.3 million vehicles in 2021 and an average of 32,000 new registrations annually (*Statistical Portal of the Valenciana, 2021*). An introduction plan is devised to analyse the implementation of the hydrogen vehicle in this location. A certain percentage of the new vehicles registered annually will be assumed to be hydrogen vehicles, starting with 1 % during the first year and contemplating three different levels according to the plan's acceptance (*Szabó et al., 2021*). The medium-rate plan with an increase of 1.5 % per year, the high-rate plan, where the percentage of new vehicles registered each year will be assumed to be hydrogen-fuelled. Moreover, the very high-rate plan, where the same will be done by 2 %. With these plans, more than 16 000 hydrogen-powered vehicles would be obtained in the case of the average acceptance of the plan, and more than 41 000 vehicles in the most favourable case, with a very high rate. In the next *Table 1*, the plan numbers are shown.



Table 1. Introduction plan description

Total cars at Valencia	1293340								
New registered cars at valencia	32386								

YEAR 1	YEAR 2	YEAR 3	YEAR 4	YEAR 5	YEAR 6	YEAR 7	YEAR 8	YEAR 9	YEAR 10
0,5%	1,5%	2,5%	3,5%	4,5%	5,5%	6,5%	7,5%	8,5%	9,5%
0,5%	2,0%	3,5%	5,0%	6,5%	8,0%	9,5%	11,0%	12,5%	14,0%
0,5%	2,5%	4,5%	6,5%	8,5%	10,5%	12,5%	14,5%	16,5%	18,5%

New H <sub>2</sub> cars									
162	486	810	1134	1457	1781	2105	2429	2753	3077
162	648	1134	1619	2105	2591	3077	3562	4048	4534
162	810	1457	2105	2753	3401	4048	4696	5344	5991

Total H <sub>2</sub> cars									
162	648	1457	2591	4048	5829	7935	10364	13116	16193
162	810	1943	3562	5668	8258	11335	14898	18946	23480
162	988	2544	4903	8147	12362	17646	24107	31861	41039

## 2.2. Hydrogen supply calculation

The necessary supply of hydrogen for implementing the plan in the society must be calculated, for which two parallel calculations have been performed so that the result has been obtained following two different procedures.

First, the starting point was a database for the consumption of traditional fuels for the fleet of private vehicles in the different provinces of Spain (*Statistical Portal of the Valenciana, 2021*). Thus, knowing the diesel and gasoline consumption for a year based on 2021 consumption, the total supply needed to provide autonomy to all vehicles in Valencia was calculated. From this, the "hydrogen energy equivalent" could be estimated, calculating the necessary hydrogen supply for vehicles in Valencia. Then, the necessary quantities for the different plans can be obtained.

Secondly, it is calculated by estimating the average distance travelled and the number of vehicles in Valencia. It is known that the average distance travelled by a private vehicle in Spain is 12562.9 km/year, and there are a total of 1 293 340 vehicles in the province of Valencia (*Statistical Portal of the Valenciana, 2021*). Thus, the quantities of traditional fuels needed to supply the entire fleet of Valencian vehicles could be calculated.

To transform the equivalent energetic quantity between traditional fuels and hydrogen, the consumptions and densities of both fuels for a given distance were calculated (*Eq 1*), obtaining a ratio of 5.6913 kg of traditional fuel for each kilogram of hydrogen. So, the required supply of hydrogen for each plan and each year can be calculated. In *Table 2*, this process is described, and following the equation, the equivalence of both fuels is calculated.

Table 2. Energetic equivalence between conventional fuels and hydrogen.

	Consumption (l/100km)	Density (kg/l)	Consumption (kg/100km)
gasoline	6	0.832	4.992
diesel	4.50	0.75	3.375
HC	5.0649	0.78	3.98
H <sub>2</sub>	-	-	0.7

$$\text{Consumption ratio} = \frac{\text{HC consumption}}{\text{H}_2 \text{ consumption}} = \frac{3,98}{0,7} = 5,6913 \quad (1)$$

In this way, the quantities needed to supply 100% of the vehicles in the province of Valencia if they were hydrogen cars are obtained in both ways, getting very similar results and with a deviation of 2.19 %, being these 111 302 t of H<sub>2</sub> with the CORES data analysis calculation and 113 625 t with the other calculation method. Given the closeness between the two methods, from now on, the author proceeded with the calculations considering the values obtained from the CORES data.



After this, from these values, the supply for each plan and each year will be calculated following Eq (2), and the results are shown in *Table 3*:

$$\text{Annual } H_2 \text{ consumption} = \text{Consumption } 100\% H_2 \text{ cars} * \frac{\text{Total } H_2 \text{ cars}}{\text{Total cars Valencia}} \quad (2)$$

Table 3. Hydrogen demand in Valencia, Spain

YEAR	Total H <sub>2</sub> Cars	H <sub>2</sub> amount(kg)	H <sub>2</sub> amount/day
YEAR 1			
0.5%	162	13935	38
0.5%	162	13935	38
0.5%	162	13935	38
YEAR 2			
1.5%	648	55741	153
2.0%	810	69677	191
2.5%	972	83612	229
YEAR 3			
2.5%	1457	125418	344
3.5%	1943	167224	458
4.5%	2429	209030	573
YEAR 4			
3.5%	2591	222965	611
5.0%	3562	306578	840
6.5%	4534	390190	1069
YEAR 5			
4.5%	4048	348384	954
6.5%	5668	487737	1336
8.5%	7287	627090	1718
YEAR 6			
5.5%	5829	501672	1374
8.0%	8258	710703	1947
10.5%	10687	919733	2520
YEAR 7			
6.5%	7935	682832	1871
9.5%	11335	975474	2673
12.5%	14736	1268116	3474
YEAR 8			
7.5%	10364	891862	2443
11.0%	14898	1282052	3512
14.5%	20905	1799053	4929
YEAR 9			
8.5%	13116	1128763	3093
12.5%	18946	1630435	4467
16.5%	28339	2438824	6682
YEAR 10			
9.5%	16193	1393534	3818
14.0%	23480	2020625	5536
18.5%	37165	3198315	8763

### 2.3. Hydrogen supply production

Once the needed hydrogen for implementing each plan has been calculated (*Table 3*), the problem of how to produce this hydrogen was investigated. To produce it, electrolysis has been selected as the most optimal process for this investigation due to its green and sustainable character. In addition, it is necessary to analyse which method best suits the project's requirements to produce the energy needed for the electrolysis process. For this, the production of the energy necessary for the hydrogen production process from solar energy was chosen, given the favourable characteristics of the Valencia location and the sustainable nature of this process. The best way to combine this is in a solar hydrogen production plant, so knowing the production needed to supply the hydrogen demanded by the FCEV (Fuel Cell Electric Vehicle - FCEVs are a type of vehicle that uses compressed hydrogen gas as fuel to generate electric power via a highly efficient energy converter, a fuel cell. The fuel cell directly transforms hydrogen into electricity to power an electric engine.) introduction plans can start with the sizing of the plant to know its approximate size. For this, the energy needed to produce one kilogram of hydrogen is known, which is 50 kWh, and knowing the efficiency ( $\epsilon$ ) of the solar panels, which is 0.21, and the average irradiance in Valencia of 5.23 kWh/m<sup>2</sup>, we can calculate approximately the size of solar panels and power needed to supply the hydrogen supply. The calculations needed are given in the 3,4,5 and 6 equations:



$$\text{Electrolysis energy}(kWh) = \frac{\text{Electrolysis energy}}{kgH_2} * H_2 \text{ amount} = 50 * H_2 \text{ amount} \tag{3}$$

$$\text{Solar energy}(kWh) = \frac{\text{Electrolysis energy}}{\epsilon} = \frac{\text{Electrolysis energy}}{0,21} \tag{4}$$

$$\text{Area}(m^2) = \frac{\text{Solar energy}}{\text{solarradiation vlc}} = \frac{\text{Solar energy}}{5,73} \tag{5}$$

$$\text{Instalated power}(kW) = \text{Solar radiation} \left(\frac{kW}{m^2}\right) * \epsilon * \text{size of solar panel} = 5.23 * 0,21 * \text{size of solar panel} \tag{6}$$

Following these steps, *Table 4* shows the results of the estimated plant size and power:

Table 4. Size and power estimation for the plant.

YEAR 1	kWh(electrolysis)	kWh(sun)	area(m2)	powinst/MW
0.5%	1909	9090	1738	0.37
0.5%	1909	9090	1738	0.37
0.5%	1909	9090	1738	0.37
<b>YEAR 2</b>				
1.5%	7636	36361	6952	1.5
2.0%	9545	45451	8690	1.8
2.5%	11454	54541	10429	2.2
<b>YEAR 3</b>				
2.5%	17181	81812	15643	3.3
3.5%	22907	109083	20857	4.4
4.5%	28634	136354	26071	5.5
<b>YEAR 4</b>				
3.5%	30543	145444	27810	5.8
5.0%	41997	199985	38238	8.0
6.5%	53451	254527	48667	10.2
<b>YEAR 5</b>				
4.5%	47724	227256	43452	9.1
6.5%	66813	318159	60833	12.8
8.5%	85903	409061	78214	16.4
<b>YEAR 6</b>				
5.5%	68722	327249	62571	13.1
8.0%	97357	463602	88643	18.6
10.5%	125991	599956	114714	24.1
<b>YEAR 7</b>				
6.5%	93539	445422	85167	17.9
9.5%	133627	636317	121667	25.6
12.5%	173715	827212	158167	33.2
<b>YEAR 8</b>				
7.5%	122173	581776	111238	23.4
11.0%	175624	836302	159905	33.6
14.5%	246446	1173550	224388	47.1
<b>YEAR 9</b>				
8.5%	154625	736310	140786	29.6
12.5%	223347	1063558	203357	42.7
16.5%	334086	1590884	304184	63.9
<b>YEAR 10</b>				
9.5%	190895	909024	173810	36.5
14.0%	276798	1318085	252024	52.9
18.5%	438125	2086311	398912	83.8

After obtaining the power required for the plans to introduce the hydrogen vehicle in Valencia, this research was continued by designing a hydrogen production plant using solar energy with a power of 10 MW, which, as shown in *Table 4*, will be possible to supply the hydrogen required for the plan during the first five years in the case of the medium rate plan or four years in the other two cases.

#### 2.4. Solar plant design for hydrogen production

The following points of the paper will analyse the technical and economic feasibility of a plant of this power to cover the designed plan. First, an analysis of the plant's annual production is carried out in a fictive location, in La Pobra de Vallobona, a small town in Valencia with a largely rural area. The following values are extracted on the solar irradiance measured as a monthly average (*Figure 1*):



## 5.23 peak sun hours per day

### Your monthly averages:

- January: 4.19
- February: 4.72
- March: 5.28
- April: 5.44
- May: 5.77
- June: 5.91
- July: 6.33
- August: 6.11
- September: 5.75
- October: 4.99
- November: 4.35
- December: 3.93

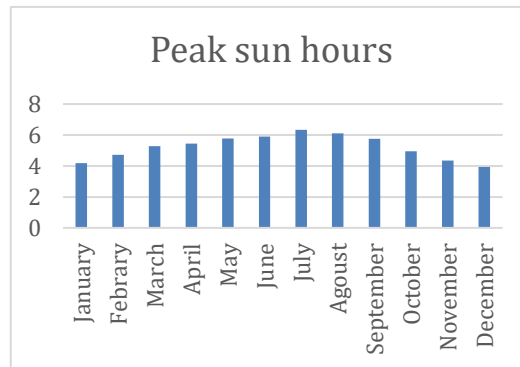


Figure 1. Monthly solar irradiation study.

Based on these data and having an installed capacity of 10 MW, the plant's maximum possible hydrogen production can be calculated. This will occur during July, with the maximum length of irradiation (*Eq. 7*):

$$Kg \text{ of } H_2 = \frac{6,33 \cdot 10000}{50} = 1266 \text{ kg/day} \tag{7}$$

To know the productive capacity of the planned hydrogen plant, the monthly production is calculated in the same way as in the previous section, analysing each month separately because the average monthly irradiation is variable. Thus, there will be months like winter in which the production will be lower. The next figures represent these calculations (*Figure 2*):

	Peak sun hrs	H <sub>2</sub> kg
January	4.19	25978
February	4.72	26432
March	5.28	32736
April	5.44	32640
May	5.77	35774
June	5.91	35460
July	6.33	39246
August	6.11	37882
September	5.75	34500
October	4.95	30690
November	4.35	26100
December	3.93	24366
Average	5.23	31817
Total	62.73	381804

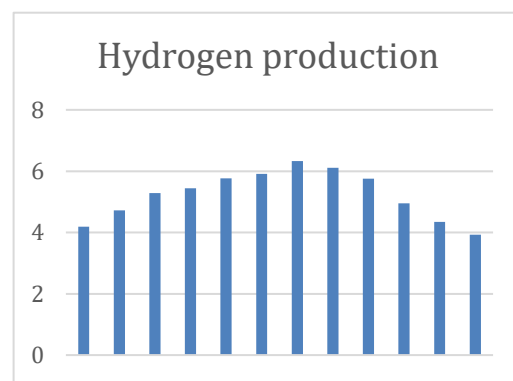


Figure 2. Hydrogen production estimation of the plant in Valencia, Spain

Therefore, with a 10 MW plant, approximately 381 t H<sub>2</sub> will be produced yearly.

### 2.5. Installation components

Thus, we already know certain technical requirements about the plant's production that will be important for further design. Further on, the most important and necessary components for the implementation of the plant will be described, and through the analysis of their cost, the author can approximate the economic viability of the implementation of this plant to supply the plan.





First, to cover the selected power, solar modules must be installed, for which the 545 W JA Solar Mono PERC model has been selected, as it is most commonly used in Spain nowadays. To reach 10 MW power, 18 349 solar panels should be installed. Thus, the total area of solar panels will be 47 500 m<sup>2</sup>. Secondly, to produce hydrogen, an electrolyser is required. This is the device with which we can carry out the electrolysis process, which consists of separating the hydrogen and oxygen molecules in water using electricity. Different electrolysers exist, such as alkaline electrolysers, proton exchange membrane electrolysers (PEM) or solid oxide electrolysers (SOEC). For this plant, the PEM electrolysers have been selected because of their benefits, which include the production of high-purity hydrogen and ease of cooling, and better performance with renewable energies due to their variable nature. To suit the size of our plant, the EL600N electrolyser from H2B2 has been selected with the following technical specifications:

### **Hydrogen gas production:**

Max. nominal hydrogen flow: 600 Nm<sup>3</sup>/h (1,290 kg/day)

Hydrogen flow range: 10–100 %

Operating pressure: 15–40 bar (217–580 psig)

Hydrogen purity (before gas purification): > 99.9 %; < 25 ppm O<sub>2</sub>; H<sub>2</sub>O saturated

Hydrogen purity (after gas purification): 99.999 %; < 5 ppm O<sub>2</sub>; < 5 ppm H<sub>2</sub>O

### **Electrical requirements:**

Power (BoP + Stacks): 3,100 kW

Stack consumption: 4.7 kWh/Nm<sup>3</sup> H<sub>2</sub>

AC power consumption (BoP + stack): 5.1 kWh/Nm<sup>3</sup> H<sub>2</sub>

### **Feed water requirements:**

Consumption: < 1 L/Nm<sup>3</sup> H<sub>2</sub>

Temperature: +5 °C to + 40 °C (+41 °F to +104 °F)

The compressor is another vital element for the installation because it transports the hydrogen at high pressures, higher than 700 bar, the pressure required in the hydrogen stations for vehicles. Two compressors, one low-pressure and one high-pressure, will be applied to achieve this. This way, the low-pressure compressor will raise the pressure to 160 bar and the high-pressure compressor to 900 bar. Therefore, the path that the hydrogen will follow in its compression process will start at the beginning of the electrolyser, from where it will be conducted to the low-pressure compressor, and after the compression process, it will be stored in the low-pressure tank at 60 bar. After this, the hydrogen will pass to the high-pressure compressor and will be stored in the high-pressure tanks, from where it can be distributed to the different hydro line plants in the province of Valencia. Thus, the equipment applied must have the above pressure requirements. In addition, the compressor must be able to work with a hydrogen flow higher than the maximum flow provided by the electrolyser, so we must look for a compressor that operates correctly with the flow required. The Hyperbaric brand was selected for this: model 1KS 50 for the first stage of compression and model 1KS 95 for the second stage, as it is widely used in Spain. Thus, two compressors will be needed for the low-pressure stage due to the high hydrogen flows and one for the high-pressure stage. Another main installation component is the low-pressure tank, where the hydrogen is stored after the first compression stage. To calculate its capacity, the daily hydrogen production must be estimated. Assuming production at 100% of the electrolyser capacity to obtain an upward estimate, which will not occur because the solar energy obtained in the most favourable month is not enough for that production level, a value of 1290 kg of H<sub>2</sub> per day is obtained. Since the pressure at the outlet of the first compression stage will be 160 atmospheres, the required tank volume can be obtained by following Eq. 8:



$$V = \frac{n \cdot R \cdot T}{P} = \frac{m \cdot R \cdot T}{M \cdot P} = \frac{1290 \cdot 0.082 \cdot 298}{0.002 \cdot 160} = 98507.6 \text{ l} \quad (8)$$

where

- $V$  is the volume [l];
- $m$  is the hydrogen mass [kg];
- $R$  is the ideal gas constant [atm-l/k-mol];
- $T$  is the temperature of hydrogen [K];
- $M$  is the molecular mass of H<sub>2</sub> [kg/mol];
- $P$  is the hydrogen pressure [atm].

For this volume, the LH 100H tank manufactured by LAPESA SL will be installed with the following technical specifications:

- Nominal volume [m<sup>3</sup>] =100
- Outer diameter D [mm]=3 000
- Overall length L [mm]=15 350
- Unladen weight [ton]=34.7

Finally, the last component that will be considered for the economic estimation of the project will be the high-pressure tank, where the hydrogen will be stored and ready for distribution. For this purpose, the required dimensions of the tank are calculated in the same way as in Eq. 7, obtaining a value of 17 512.5 l.

After that, the LH 25H model is selected with the following technical data:

- Nominal volume [m<sup>3</sup>] =25
- Outer diameter D [mm]=2 200
- Overall length L [mm]=7 850
- Unladen weight [ton]=10.1

Now, the main components of the solar hydrogen production plant are known, and the economic analysis can be performed.

### 3. Results and discussion

#### 3.1. Economic viability analysis.

In order to be able to make the feasibility study of this project, the different types of costs that the implementation of the hydrogen production plant would carry and the income generated by the sale of the hydrogen at the different points of distribution and sale to the public must be analysed.

Firstly, the different fixed costs will be collected, mainly the investment in the equipment necessary to construct the hydrogen production plants. In addition, other fixed costs will be the purchase of the building and the land. These costs are represented in Table 5:



Table 5. Fixed costs.

Fixed costs			
Equipment [€]	Units [€]	Unit price [€]	Amount [€]
Solar panels 545W JA Solar Mono PERC	18349	216.24	3967788
Electrolyzer EL600N H2B2	1	10000000	10000000
Compressor 1KS50	2	500000	1000000
Compressor 1KS95	1	600000	600000
Low-pressure tank	1	98900	98900
High-pressure tank	1	253100	253100
Land and warehouse purchase	1	300000	300000
	Total		16219788

In addition, the different variable costs of the installation must also be considered. These include the costs for the water supply of the electrolyser, and an average water price of 1.97 €/m<sup>3</sup> will amount to 15,000 €. A small percentage of the project's direct costs must be established destined to the complementary direct costs, which include concepts that are difficult to quantify. Thus, we will establish 1% of direct costs. Also, indirect costs are execution costs not attributable to specific work units but to the whole or part of the project. For these, we establish 4% of the direct costs. An example of these costs would be plant maintenance. The Budget for Material Execution and the Investment Budget can be calculated by applying the different standardised rates (Table 6):

Table 6. Investment budget.

Equipment [€]	Units [€]	Unit price [€]	Amount [€]
Solar panels 545W JA Solar Mono PERC	18 349	216	3 967 788
Electrolyzer EL600N H2B2	1	10 000 000	10 000 000
Compressor 1KS50	2	500 000	1 000 000
Compressor 1KS95	1	600 000	600 000
Low-pressure tank	1	98 900	98 900
High-pressure tank	1	253 100	253 100
Land and warehouse purchase	1	300 000	300 000
Water yearly supply	20	750	15 000
Equipment and material budget			16 234 788
Complementary direct costs (1%)			162 348
Indirect costs (4%)			649 392
(1) Budget for Material Execution (1)			17 046 527
(2) Overhead Expenses (0,13*1)			2 216 049
(3) Industrial Profit (0,06*1)			1 022 792
(4) Contract execution budget (1+2+3)			20 285 367
(5) Value added tax (0,21*4)			4 259 927
(6) Investment Budget (4+5)			24 545 294

The hydrogen plant's income will come from selling hydrogen to the different hydrogen sales points. Thus the selling price of a kilogram of hydrogen must be known. Due to the current uncertainty about the price of hydrogen, to investigate the feasibility, instead of setting a specific price, it was calculated from what price our project starts to be profitable. Graphically this can be understood as the intersection between the cost and benefit curve, and the point of the intersection is called the break-even point. We must draw both curves from the data to translate this to the present case. First, the cost curve can be approximated to the fixed costs since the variable costs only include the water supply, and their cost is insignificant to the investment budget. So the cost will be represented by a straight line with the value of the investment cost. In addition, due to the lack of data on the residual value of the installation components, we will be in the most unfavourable situation to avoid failing the feasibility study, and we will take the residual values of the acquired equipment as 0. Second, the income curve is studied. This has a higher complexity since the selling price of hydrogen, as mentioned above, is very uncertain for the coming years. It is expected that with economies of scale, it will be reduced considerably. Therefore, we cannot determine the slope of the income curve and plot the situation to find the break-even point.

Due to this, the minimum average selling price of hydrogen will be calculated so that the investment is recovered in the 20 years of the project's useful life. It will be studied if it fits with the predictions that exist or, on the contrary, it is an unreal price, and therefore the project of the construction of the plant to supply green hydrogen for the plan of introducing vehicles would not be viable.



After these calculations, we obtain an average selling price of hydrogen of 3.21 €, from which the investment will be recovered in 20 years. The following graphs represent the break-even points for a price of 3.21 €/kg H<sub>2</sub> and 5 €/kg H<sub>2</sub>, with the amount in € on the y-axis and the years since start-up on the x-axis. 100% production capacity of the plant is assumed, so 381 t H<sub>2</sub> are produced each year (Figure 3):

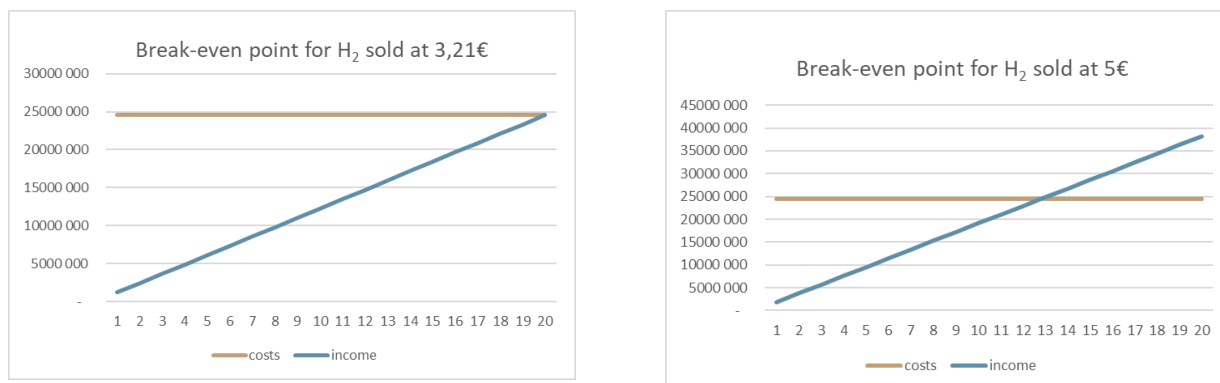


Figure 3. Break-even point graph for H<sub>2</sub> price of 3.21 and 5€.

As can be seen in the first graph, if the plant operates at 100 % and the average selling price of hydrogen during the investigation period is 3.21 €, the investment will be recovered in year 20, while if the price of H<sub>2</sub> is increased to 5 €, the investment will be recovered in year 12, and the useful life of the plant will end with an approximate profit of 15 million €. Considering the hydrogen market and the predictions we found about its price in the future, we can see that currently, its selling price is 8 to 10 €. However, due to economies of scale, there will be a considerable reduction in the prices of fuel cells and storage tanks, which will bring about a 70 % reduction in the cost of hydrogen production over the next ten years. A comparative analysis between hydrogen and other conventional fuels can be analysed to get a different perspective on the selling price of hydrogen and whether it would be attractive to the market. For this, the costs of the equivalent amount of energy in terms of autonomy in both cases and the percentage difference between the two prices will be the energetic equivalent in terms of the autonomy of 1 kg of H<sub>2</sub> is 7.2965 litres of traditional fuels and setting an average price of 1.795 €/l, the total price for this amount of energy is 13.1 €, a value much higher than that obtained for hydrogen in the study, which put its selling price of that amount of energy between 3.21 and 5 €. In percentage terms, hydrogen would give us a 62 % cheaper energy to power vehicles. This saving can be observed more clearly when the price is analysed as a function of the kilometres travelled. Acting in this way, the price for travelling 100 km with an H<sub>2</sub> vehicle and considering a high consumption value for hydrogen vehicles, would oscillate between 3.21 and 5 € due to the range of sales prices with which we have been working in this study while using conventional fuel would be 9.1 €/100 km.

### 3.2. Environmental viability analysis.

The benefits of implementing the studied plan can also be addressed from an environmental point of view. For this, when analysing the reduction of pollutant emissions, only the previous emissions of vehicles with conventional fuels should be calculated since the saving will be 100%. The analysis of environmental data on vehicle emissions during the year 2021 proves that vehicles emit an average of 2.45 kg of CO<sub>2</sub> per litre of fuel, so knowing the litres of fuel that will be saved with the implementation of the plan can be known the savings of CO<sub>2</sub> emissions into the atmosphere. After these simple calculations, we obtain values of a reduction of CO<sub>2</sub> emissions close to 200 000 megagrams after the 10-year duration of the plan. Lastly, the economic value of these emissions can be determined. The price of CO<sub>2</sub> emission allowances during 2021 reached an annual average of 53.55 €/t, so we multiplied this value by the calculated emissions to obtain the economic value of 10 710 000 €.

### 4. Conclusion

In conclusion, after studying the sustainable plan for introducing hydrogen vehicles in the province of Valencia, it has been possible to show the strong advantages that the implementation of hydrogen technologies can bring to the automotive industry, and the barriers are to be dealt with. A proposed plan covers the sale of hydrogen vehicles and the calculation of the required hydrogen fuel supply for the sustainable production of hydrogen fuel, showing the necessity of the progressive electrification of the automotive market and the consequent evolution of hydrogen production systems to supply this change in the market. After this study, the feasibility of this project has become clear after analysing the approximate investment cost of a fully green hydrogen production plant, the implementation of which will be a key point in the course towards sustainable hydrogen. Also, the economic and environmental benefits of this change in the vehicle market have been discussed, and the beneficial character of introducing the studied plan has been evidenced. In addition, it must be emphasised the stage of development of the hydrogen market and how economies of scale will make hydrogen prices even more competitive. This is a technology whose future will undoubtedly be very promising.



## References

- Ágoston, G., Madleňák, R. (2021). Road safety macro assessment model: Case study for Hungary. *Periodica Polytechnica Transportation Engineering*. 49(1), 89–92. DOI: <https://doi.org/kj2c>
- Andrejszki, T., Torok, A., Csete, M. (2015). Identifying the utility function of transport services from stated preferences. *Transport and Telecommunication Journal*. 16(2), 138–144. DOI: <https://doi.org/gm39>
- Szabó, Z., Török, Á., Sipos, T. (2021). Order of the cities: Usage as a transportation economic parameter. *Periodica Polytechnica Transportation Engineering*. 49(2), 164–169. DOI: <https://doi.org/gt43>
- Statistical Portal of the Valenciana (2021). URL: <https://pegv.gva.es/es/estad%C3%ADstica-del-parc-nacional-de-vehiculos>
- Torok, A., Torok, A., Heinitz, F. (2014). Usage of production functions in the comparative analysis of transport related fuel consumption. *Transport and Telecommunication*. 15(4), 292. DOI: <https://doi.org/h8zm>
- Szendrő, G., Csete, M., & Török, Á. (2012). Statistical analysis of the road vehicle fleet of Hungary from environmental aspects. *Periodica Polytechnica Transportation Engineering*, 40(2), 95-98. DOI: <https://doi.org/gn86xv>
- Zalacko, R., Zöldy, M., Simongáti, G. (2021). Comparison of alternative propulsion systems. A case study of a passenger ship used in public transport. *Brodogradnja: Teorija i praksa brodogradnje i pomorske tehnike*. 72(2), 1–18. DOI: <https://doi.org/kj2b>
- Zöldy, M. (2009). Automotive industry solutions in response to European legislative emission regulation challenge. *Mokslas–Lietuvos ateitis/Science–Future of Lithuania*. 1(6), 33–40. DOI: <https://doi.org/chhr44>